NASA CR — 54955

THIRD QUARTERLY REPORT

DEVELOPMENT OF HIGH-PERFORMANCE LIGHT-WEIGHT ELECTRODES

FOR HYDROGEN-OXYGEN FUEL CELLS

by

D. Gershberg, Principal Investigator

W. P. Colman
J. DiPalma

prepared for

NATIONAL AERONAUTICS AND SPACE ADMINISTRATION

May 15, 1966

CONTRACT NAS 3-6477

Period Covered: October 6, 1965 - January 5, 1966

NASA Lewis Research Center
Cleveland, Ohio
Space Power Systems Division
Technical Manager: Mr. Meyer R. Unger

AMERICAN CYANAMID COMPANY
STAMFORD RESEARCH LABORATORIES
1937 West Main Street
Stamford, Connecticut 06904
(Area Code 203) 348-7331

TABLE OF CONTENTS

TABLE OF CONTENTS

(Continued)

LIST OF TABLES

LIST OF FIGURES

1. INTRODUCTION

1.1 Objectives

Light-weight fuel batteries capable of producing large
quantities of energy appear feasible for space applications. High-
performance light-weight electrode systems are an essential part of
these batteries. Work completed previously[1], under NASA Contract
NAS 3-2786, showed that American Cyanamid AB-40 electrodes (40 mg Pt/cm^2)
give high and sustained performance in hydrogen-oxygen matrix fuel cells
including those of battery size; this performance is substantially higher
than that of American Cyanamid AB-1 electrodes which contain less platinum
(9 mg Pt/cm^2). It was calculated that at temperatures up to 100°C, the
AB-40 electrodes could be incorporated in a 2 kw fuel battery whose
weight per net power (including all auxiliaries except fuel and tankage)
would be approximately 50 lb/kw.

A detailed investigation at temperatures up to 100°C showed
that initial performance generally increases with increasing temperature,
pressure, and electrolyte (KOH) concentration. Furthermore, preliminary
studies demonstrated that substantial increases in initial performance
can be obtained by operating at higher temperatures (140°C) and KOH
concentrations (65%), than are generally employed in matrix fuel cells.
Under these conditions current densities as high as 100, 400 and 800 ma/cm^2
at working voltages of 1.0, 0.9 and 0.8 v, respectively, were achieved
in short term tests.

Accordingly the objective of the present contract is to
investigate and recommend preferred conditions, at 100-200°C under
which AB-40 electrodes would be capable of sustained high performance
in a total module having a weight-to-power ratio substantially lower
than those presently available for space environment.

1.2 Scope

The scope of work to be done by American Cyanamid Company during the Contract year is outlined in the Schedule of Work presented in the First Quarterly Report[2].

Work in the third quarter of the contract was devoted to Tasks I-A, I-B, and III. In Task I-A, the initial performance and short term stability of a ceria-PTFE matrix were evaluated. An empirical model of pressure-temperature-KOH concentration effects on initial performance was developed from a computer analysis of data reported in the second quarter. The effect on initial performance of the fraction of product water removed at each electrode was investigated. In Task I-B, small cell life tests were conducted, primarily with asbestos matrices. Large cell life testing was continued (Task III).

2. SUMMARY

Task I-A

1. An experimental Ceria-PTFE matrix was found to have a combination of low resistivity (2.0 ohm-cm at 100°C and 50% KOH) and high bubble pressure (16-20 psig) superior to all matrices evaluated earlier. As reported previously[3], this type of matrix also has good corrosion resistance to KOH at temperatures up to at least 150°C though not at 200°C. At atmospheric pressure, the maximum initial performance of the electrode obtained with this matrix at 100 ma/cm^2 was 0.98 v, 1.03 v and 1.07 v at 100°C, 150°C and 200°C, respectively. At 400 ma/cm^2 the maximum initial voltages were 0.87 v, 0.88 v and 0.96 v at these same respective temperatures.

2. Several short term tests with the Ceria-PTFE matrix were conducted, in one-inch cells, mostly at 150°C and 100 ma/cm^2. Rapid voltage decline rates (15-400 mv/100 hrs.) occurred during operation with either dry gases or with one gas humidified substantially. Stable operation was demonstrated in one run at 150°C for 20 hours at a voltage of 1.00 v, though not for longer periods. Humidification of both inlet gases may be necessary for long term stability. The ceria-PTFE matrix is to be included in the life-testing program.

3. An empirical model for the dependence of initial performance on temperature (100-150°C), pressure, (0-60 psig), and KOH concentration (30-75%) was fitted to experimental data reported during the Second Quarter. The model permits predictions of cell voltage to within ± 5-15 mv at 100-400 ma/cm^2, though not at 600-1000 ma/cm^2.

The effects of the operating variables on initial performance predicted by the model confirm the preliminary conclusions, based on direct analysis of the data, which were reported during the second quarter[3]. For the region of operating variables studied, highest initial performance is predicted at 150°C, 45-60 psig and, depending on the current density, 60-75% KOH. Highest predicted working voltages are 1.10 v, 1.04 v, 0.99 v and 0.95 v at 100, 200, 300 and 400 ma/cm^2, respectively.

Matrices which are less resistive or thinner than that used to obtain the data (16-18 mil ACCO-II Asbestos) might increase this performance by as much as 30 mv at 100 ma/cm^2 and 100 mv at 400 ma/cm^2.

4. The effect of the fraction of water removed at each electrode on initial performance was studied with an ACCO-II Asbestos matrix operating on dry gases. At 100-200 ma/cm^2, highest initial voltages were obtained by removing all product water at the hydrogen electrode. By contrast, highest performance at 600-1000 ma/cm^2 occurred when two-thirds or more of the product water was removed at the oxygen electrode. At 300-400 ma/cm^2 the initial performance was independent of this variable.

Task I-B

1. Most small cell life tests were carried out in 2-inch cells at 100°C, 50% KOH, and atmospheric pressure. Both dry and humidified reactant gases were employed.

2. Stable electrode operation was obtained for more than 1200 hours at a current density of 100 ma/cm^2, using either ACCO-I Asbestos or Fuel Cell Asbestos as the matrix. Quinterra Asbestos has yielded stable performance for at least 429 hours. Cell voltages at 100 ma/cm2 were generally in the range 0.92-0.94 v.

3. At 200 ma/cm^2, pressure tests were run at 15 psig on dry gases using either ACCO-I Asbestos or Fuel Cell Asbestos as the matrix. Thus far, performance stability has at best been borderline. Further pressure tests are to be run with humidified gases.

4. Stable electrode performance was also achieved for more than 1200 hours at 300 ma/cm2 with ACCO-I Asbestos as the matrix. Cell voltages were mostly 0.86-0.88 v.

5. ACCO-II Asbestos and Fuel Cell Asbestos have not yet yielded stable performance at 300 ma/cm^2. This may be due to the relatively high electrolyte concentration gradients which developed across these matrices.

6. Long term performance at 100-300 ma/cm2 was stable when the overall KOH concentration gradient in the cell was below 6-7% KOH. Unstable operation occurred when this gradient was 7-15%.

The concentration gradient increased with increasing current density and decreased with decreasing density of the matrix in the order Fuel Cell Asbestos (2.5-15% KOH), ACCO-II Asbestos (0.5-10.0% KOH), and ACCO-I Asbestos (0.5-7.5% KOH). At high current density (300 ma/cm^2) humidification of the inlet gases reduced the concentration gradient by 3-4% KOH.

7. Long term stability has not yet been attained at 400 ma/cm^2. However, stable operation obtained for a limited period (320 hours) offers promise for long term stability at this current density.

8. Tests at 125°C confirmed previous results that asbestos and PTFE-asbestos matrices are unsuitable for long term stability at this temperature.

9. Two tests at 150°C with a commercial porous PTFE as the matrix immediately developed cross leakage of gas and were terminated.

Task III

1. Testing of battery-size electrodes was conducted in a 6-inch cell at 100°C, 50% KOH and atmospheric pressure. The matrix was ACCO-I Asbestos. The removal of product water simulated that of a battery system with a recycle hydrogen stream and dead-ended oxygen. Stable performance was achieved at 300 ma/cm^2 for 740 hours at a voltage of 0.85-0.87 v and a voltage decline rate of 1.2 mv/100 hours. Inadvertent overwetting during 740-850 hours caused a sharp voltage decline. Despite this the total voltage decline (49 mv) after 1000 hours of operation passed contract specifications.

3. SMALL CELL TESTING

3.1 Investigation of Matrix Materials: Ceria-PTFE

An experimental proprietary ceria-PTFE matrix containing 95% ceria by weight (85% by volume) is under investigation. Previously reported corrosion data[3] indicate that this type of matrix may be suitable for sustained operation at temperatures up to at least 150°C, though not at 200°C. This matrix has a bubble pressure of 16-20 psig, nearly as high as that of ACCO-II Asbestos and Fuel Cell Asbestos (20 to 30[+] psig), and considerably higher than that of ACCO-I Asbestos (1-3 psig). It should, therefore, be useful at pressures above atmospheric.

The matrix as prepared is saturated with water and has a void volume of approximately 80%. On drying, the matrix shrinks and suffers a loss in porosity which is not fully recoverable on re-equilibration in KOH. To avoid this loss in porosity, the water-wet matrices are not dried, but are transferred directly to the 50% KOH solution. The maximum electrolyte loading obtainable in this manner, as calculated from a void volume of 80%, is 0.86 g KOH solution/g dry matrix.

Cell resistance and initial electrode performance with 18-20 mil thick ceria-PTFE matrices were studied at 100-200°C. KOH loadings were varied over the range 25-100% of the maximum, the lower values being obtained by blotting the fully-loaded matrix. Table 3-1 compares the cell resistance and initial performance of the ceria-PTFE matrix with that of asbestos matrices and shows their dependence on KOH loading.

Cell: One Inch
Electrodes: AB-40
Pressure: 0 psig

TABLE 3-1

Initial Performance of Ceria-PTFE Matrix at 100-200°C

Matrix	Temp. (°C)	KOH Conc. Wt. (%)	KOH Loading Fraction (of Maximum)	Cell Resistance (Ohms)	Working Voltage at Current Density (ma/cm^2) of:						
					100	200	300	400	600	800	1000
Ceria-PTFE	100	50	.25	.012	.98	.93	.90	.87	.80	.70	+
Ceria-PTFE	100	50	.50	.018	.94	.88	.83	.77	+		
Ceria-PTFE	100	50	.75	.017	.89	+					
Ceria-PTFE	100	50	1.00	.018	.89	+					
ACCO-I Asbestos (a)	100	50	-	.018	.98	.93	.90	.88	.82	.76	.72
ACCO-II Asbestos (a)	100	50	-	.032	.96	.91	.87	.83	.75	.65	.52
Fuel Cell Asbestos (a)	100	50	-	.037	.96	.91	.86	.81	.73	.65	.57
Ceria-PTFE	150	67	.25	.026	1.03	.98	.93	.88	.78	.66	.53
Ceria-PTFE	150	67	.50	.026	1.03	.98	.92	.87	.75	.65	.50
Ceria-PTFE	150	67	.75	.035	1.03	.98	.92	.87	.75	.60	.46
Ceria-PTFE	150	67	1.00	.025	1.03	.98	.91	.81	.61	+	
Ceria-PTFE	200	75	1.00	.016	1.07	1.02	.99	.96	.88	.79	.64

(a) Reported previously[2]
+ Unstable

At 100°C and 50% KOH the resistance of the ceria-PTFE matrix (0.012-0.018 ohm) equalled or was lower than the same thickness of ACCO-I Asbestos (0.018 ohm), and was substantially below that of ACCO-II Asbestos (0.032 ohm) and Fuel Cell Asbestos (0.037 ohm). The initial performance at 100°C improved markedly as the KOH loading was reduced below the maximum. At maximum loading, 0.75 maximum, and 0.50 maximum, the initial performance was far below that of asbestos matrices and was unstable at current densities above 100-400 ma/cm^2. (This instability and the improvement in performance as the loading was reduced show that the electrodes were overwet at these loadings.) At 0.25 maximum loading, the performance equalled that of ACCO-I Asbestos at current densities up to 600 ma/cm^2 and was significantly higher than that of ACCO-II Asbestos and Fuel Cell Asbestos at current densities up to 800 ma/cm^2. The working voltage was 0.98 v at 100 ma/cm^2 and 0.87 v at 400 ma/cm^2.

At 150°C and 67% KOH the performance was independent of initial KOH loading over the range 0.25 maximum-maximum at current densities up to 300 ma/cm^2. At 400-1000 ma/cm^2, the performance increased significantly as the loading was decreased without any consistent change in cell resistance. The highest working voltages obtained at 100 and 400 ma/cm^2 were 1.03 v and 0.88 v respectively.

At 200°C, 75% KOH, and maximum loading the voltages obtained at 100 and 400 ma/cm^2 were respectively 1.07 v and 0.96 v. This initial electrode performance was the same as that reported previously[2] at 200°C with a PTFE-Asbestos matrix.

Thus the ceria-PTFE matrix has a combination of low resistivity (2.0 ohm-cm) and high bubble pressure (16-20 psig) superior to that of any of the asbestos matrices evaluated thus far in this investigation. This gives it a potential performance advantage over these asbestos matrices for operation under pressure. A second potential advantage of the ceria-PTFE matrix is its possible use at temperatures substantially above 100°C, the approximate maximum temperature suitable for asbestos matrices[3]. This would permit increases in the initial performance.

Accordingly short term stability tests were run on the ceria-PTFE matrix. The tests were conducted in one-inch cells at 150°C, 67% KOH and 100 ma/cm^2, for periods of 42-95 hours. The initial KOH loading and the humidity of the inlet gas streams were varied. In all tests two thirds of the product water was removed at the hydrogen electrode. Results are shown in Table 3-2.

Initial voltages ranged mostly from 1.00 to 1.03 v. When dry gases were employed at initial KOH loadings of 0.50-0.75 maximum, the voltage decline rates (152-400 mv/100 hrs.) were extremely high (tests 7556-181 and -186). In these runs the cell resistance rose by 18-26 milliohms which indicates that portions of the electrodes may have dried out. To minimize drying at the hydrogen electrode, tests 7556-194 was run with the inlet hydrogen stream humidified at 55°C. In principle this prevented the KOH concentration at the hydrogen electrode from exceeding 71%, which is 9% below the solubility limit at 150°C. The inlet oxygen was humidified only slightly at 25°C. The KOH loading was 0.25 maximum. As with the dry gas runs, the cell resistance rose by 22 milliohms and the voltage declined very rapidly (304 mv/100 hours).

TABLE 3-2

Short Term Tests of Ceria-PTFE Matrix

Cell: One Inch
Electrodes: AB-40
Pressure: 0 psig

Test	Temp. (°C)	KOH Conc. (Wt. %)	Initial KOH Loading (Fraction of (c) Maximum)	Inlet Condition of: Hydrogen	Oxygen	Fraction of Product Water Removed At Hydrogen Electrode	Test Duration (Hrs.)	Working Voltage Initial	Final	Overall Voltage Decline Rate (mv/100 hrs.)	Cell Resistance (Ohms) Initial	Final
7556-18[a]	150	67	0.75	Dry	Dry	0.67	95	1.012	.867	152	.038	.056
7556-186[a]	150	67	0.50	Dry	Dry	0.67	42	1.030	.860	400	.026	.052
7556-194[a]	150	67	0.25	Humidified at 55°C	Humidified at 25°C	0.67	44	1.034	.900	304	.026	.048
7676-6	150	67	0.50	Humidified at 25°C	Humidified at 55°C	0.67	20 / 45	1.001 / .998	.998 / .975	15 / 92	.026 / .030	.030 / .070
7676-20[b]	150	67	0.50	Humidified at 25°C	Humidified at 55°C	0.67	42	.979	.935	104	.071	.098
7676-1[a]	100	50	0.25	Dry	Dry	0.67	137	.985	.930	40	.018	--

(a) Two polarization curves run to 1000 ma/cm² before test started.

(b) Matrix exposed to 70% KOH at 150°C for 100 hours before test.

(c) Approximately 1.4 cc KOH/cc Dry Matrix

The most stable short term operation was obtained by minimizing drying at the oxygen electrode (7676-6). The inlet oxygen stream was humidified at 55°C while the inlet hydrogen was humidified only slightly at 25°C. The KOH loading was 0.50 maximum. During the first 20 hours the cell resistance increased by only 4 milliohms and the voltage dropped only 3 mv. The voltage decline rate was 15 mv/100 hours. During the next 25 hours the resistance rose by 40 milliohms and the voltage decline rate increased to 97 mv/100 hours. The test indicated that substantial humidification of the inlet oxygen stream may be necessary for stability.

An attempt was made to determine whether any KOH-soluble impurities in the martix might be causing the voltage declines observed in these short term tests. Accordingly, a matrix sample was extracted in 70% KOH at 150°C for 100 hours and then washed with water prior to the test (7676-20). This treatment shrank the matrix somewhat and probably was the cause of a high initial cell resistance (0.071 ohm) and a relatively low initial voltage (0.979 v). The test was run with oxygen humidified at 55°C. During 42 hours the cell resistance rose by 27 milliohms and the voltage declined rapidly (104 mv/100 hours). The similarity of these results to those for unextracted matrices might indicate that lack of stability was not caused by matrix impurities. However, the matrix shrinkage caused by the extraction is a complicating factor.

One test (7676-1) was run at 100°C, 50% KOH and 100 ma/cm^2 on dry gases. The KOH loading was 0.25 of the maximum. The initial voltage was 0.985 v. During 137 hours the overall voltage decline rate (40 mv/100 hours) was high but was considerably below that of the runs made at 150,C with dry gases (7556-181 and -186).

The stability obtained during 20 hours in test 7676-6 is encouraging and the ceria PTFE matrix is to be included in the life-testing program. The short term tests indicate that, at this high KOH concentration, local drying in the electrodes may be a cause of the rapid voltage declines observed. Accordingly life tests will be run with both gases substantially humidified. Tests will be run at 100°C as well as at higher temperatures.

3.2   Investigation of Operating Variables

3.2.1   Empirical Models for Temperature-Pressure KOH Concentration Effects

Statistically-designed experiments to determine the dependence of initial electrode performance on temperature (100-150°C), pressure (0-60 psig) and KOH concentration (30-75%) were completed during the Second Quarter[3]. (A total of 27 independent runs were made, at 100-1000 ma/cm^2, at different combinations of the operating variables. Three replicate runs were made at a point near the center of the design. All runs employed ACCO-II Asbestos (16-18 mils) as the matrix.)

In order to predict the initial voltage at any point in this region of the four operating variables, (including current density) two empirical models were formulated to fit the data and computer solutions of these models were obtained.

3.2.1.1 Direct Model

A "direct model" was formulated first by considering directly the total effect of the operating variables on cell voltage. The model is based on a complete third order equation containing 35 terms with

constant coefficients. In order to solve for the coefficients, eight
of the third order terms were eliminated so that the number of coefficients
equals the number of independent experimental runs. The model is shown
in equation (1).

$$V = b_0 + b_1 K + b_2 P + b_3 C + b_4 T +$$

$$b_{11}(K)^2 + b_{22}(P)^2 + b_{33}(C)^2 + b_{44}(T)^2$$

$$+ b_{12} K P + b_{13} K C + b_{14} K T$$

$$+ b_{23} P C + b_{24} P T + b_{34} C T \tag{1}$$

$$+ b_{111}(K)^3 + b_{222}(P)^3$$

$$+ b_{112}(K)^2 P + b_{114}(K)^2 T$$

$$+ b_{221}(P)^2 K + b_{224}(P)^2 T$$

$$+ b_{331}(C)^2 K + b_{332}(C)^2 P + b_{334}(C)^2 T$$

$$+ b_{441}(T)^2 K + b_{442}(T)^2 P$$

$$+ b_{124} K P T$$

where: V = cell voltage (volts)

$$K = \frac{K'-45}{10}$$

$$P = \frac{P'-30}{10}$$

$$T = \frac{T'-125}{25}$$

$$C = \frac{C'-100}{100}$$

b = constant coefficient

and K', P', T' and C' are respectively KOH concentration (%), pressure (psig), temperature (°C) and current density (ma/cm^2).

The magnitudes of the coefficients were estimated from the simultaneous equations generated by the experimental runs. The method of least squares was used to find the set of coefficients which minimizes the sum of the squared deviations of the observed voltages from the voltages predicted by the equation. The coefficient values are shown in Table I of the Appendix. With this set of coefficients the standard deviation of the actual voltages from the predicted voltages is 10 mv at current densities of 100-400 ma/cm^2 and 23 mv at 600-1000 ma/cm^2. Both of these standard deviations are substantially higher than the experimental error (4 mv) determined by the replicate measurements. Accordingly, this model does not fit the data well.

3.2.1.2 Indirect Model

A better fit of the data is obtained by an "indirect model" which combines an equation for the dependence of cell voltage on all of the operating variables and on cell resistance, with a separate equation for the dependence of cell resistance on the operating variables.

The voltage equation, (2), is a full second order equation of the form.

$$V = b_0 + [b_1 K + b_2 P + b_3 C + b_4 T + b_5 R]$$

$$+ \quad b_{11}(K)^2 + b_{22}(P)^2 + b_{33}(C)^2 + b_{44}(T)^2 + b_{55}(R)^2$$

$$+ b_{12}K P + b_{13}K C + b_{14}K T + b_{15}K R$$

$$+ b_{23}P C + b_{24}P T + b_{25}P R \tag{2}$$

$$+ b_{34}C T + b_{35}C R$$

$$+ b_{45}T R$$

where R = cell resistance (ohms) and the other terms are as in equation (1).

The magnitudes of the coefficients were evaluated, from simultaneous equations generated by the experimental data, by the method of least squares and are shown in Table II of the Appendix. With this set of coefficients, the standard deviation of the predicted voltages from the observed voltages is 7 mv at current densities of 100-400 ma/cm^2 and 22 mv at 600-1000 ma/cm^2.

The resistance equation is a full second order equation in terms of temperature, KOH concentration, and pressure. While in principle pressure should not affect cell resistance it is included as a variable because of its apparent effect on cell resistance in the experimental runs. The resistance equation, (3), has the form:

$$R = d_0 + [d_1 K + d_2 P + d_3 T] + \tag{3}$$

$$[d_{11}(K)^2 + d_{22}(P)^2 + d_{33}(T)^2 + d_{12}K P + d_{13}K T + d_{23}P T]$$

The coefficients were calculated from the data by the method of least squares and are shown in Table III of the Appendix. The standard deviation of the predicted resistance from the actual resistance is .0052 ohm.

Cell voltages were then predicted by substituting the resistance values predicted by equation (3), into equation (2). The standard deviation of these predicted voltages from the observed voltages is 8 mv at 100-400 ma/cm^2 which is substantially closer to the duplicate measurement error than that of the direct model. Accordingly, the indirect

model is used for predicting the cell voltage at 100-400 ma/cm^2.
The model is satisfactory in this current density range. The 95% confidence limits for the predicted voltages range from $\pm$ 5 mv near the center of the design (125°C, 45% KOH, 30 psig) to $\pm$ 15 mv near the extremities (100°C, 30% KOH, 0 psig and 150°C 75% KOH, 60 psig).

The model does not give a good fit of the data at 600-1000 ma/cm^2. At these current densities the estimated standard deviation (24 mv) is much higher than the experimental error. The 95% confidence limits are at least $\pm$ 15 mv in the center of the design and at least $\pm$ 45 mv at the extremities. At present, this does not seriously limit the usefulness of the model since long term stability at these current densities generally has not yet been demonstrated for fuel cell electrodes. The current density range in which the model is satisfactory is of much more immediate interest for fuel batteries.

Figures 3-1, 3-2, and 3-3 show voltages predicted for AB-40 electrodes at physically feasible conditions within the region 100-150°C, 30-75% KOH and 0-60 psig, at current densities of 100, 200 and 400 ma/cm^2. These plots permit an estimate of the voltage at any point in the region at KOH concentrations up to 5% below the solubility limit. Values at 300 ma/cm^2 can be obtained by linear interpolation.

EMPIRICAL MODEL

PERFORMANCE vs. PRESSURE
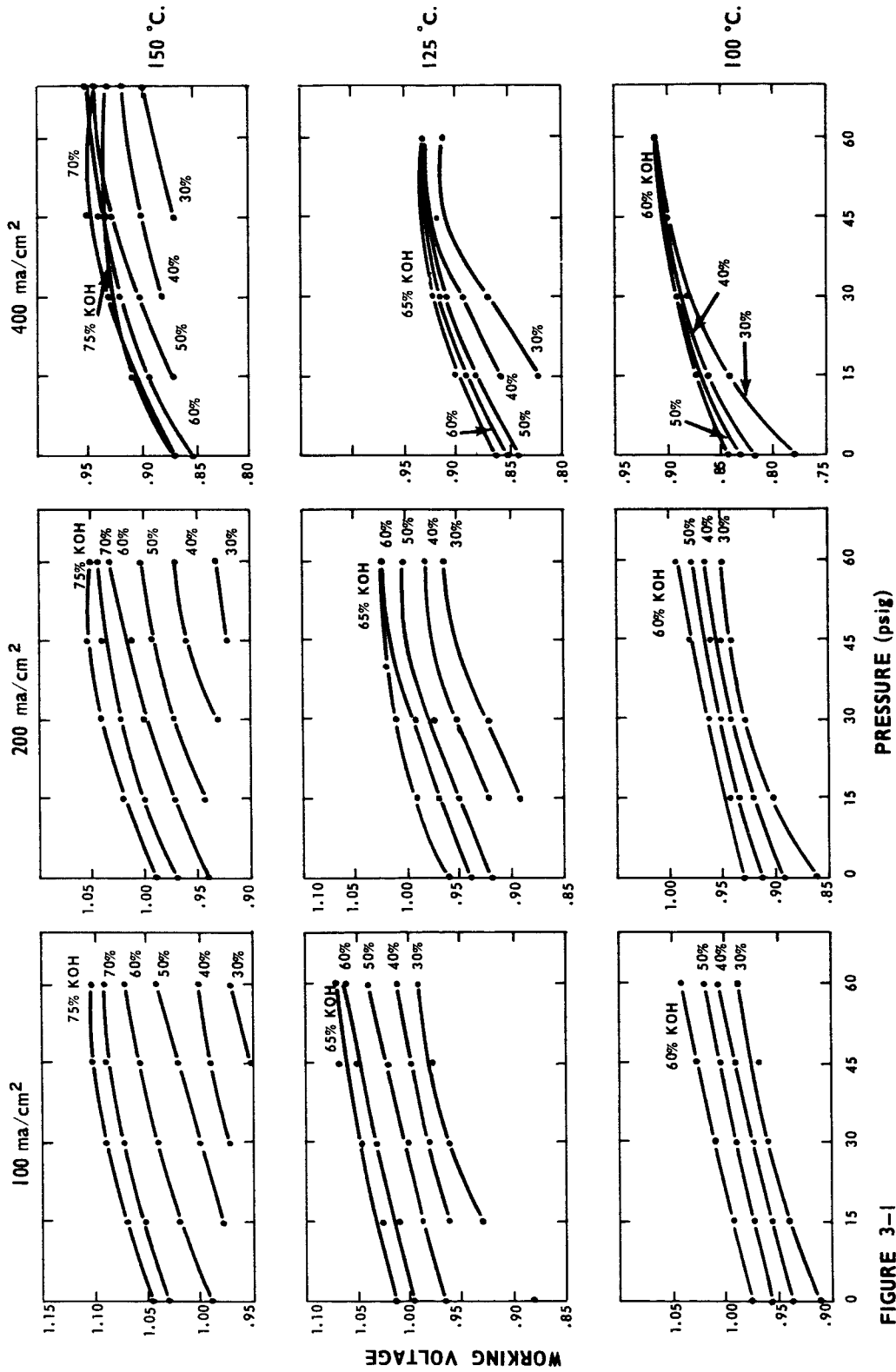
FIGURE 3-1

EMPIRICAL MODEL
PERFORMANCE vs. KOH CONCENTRATION
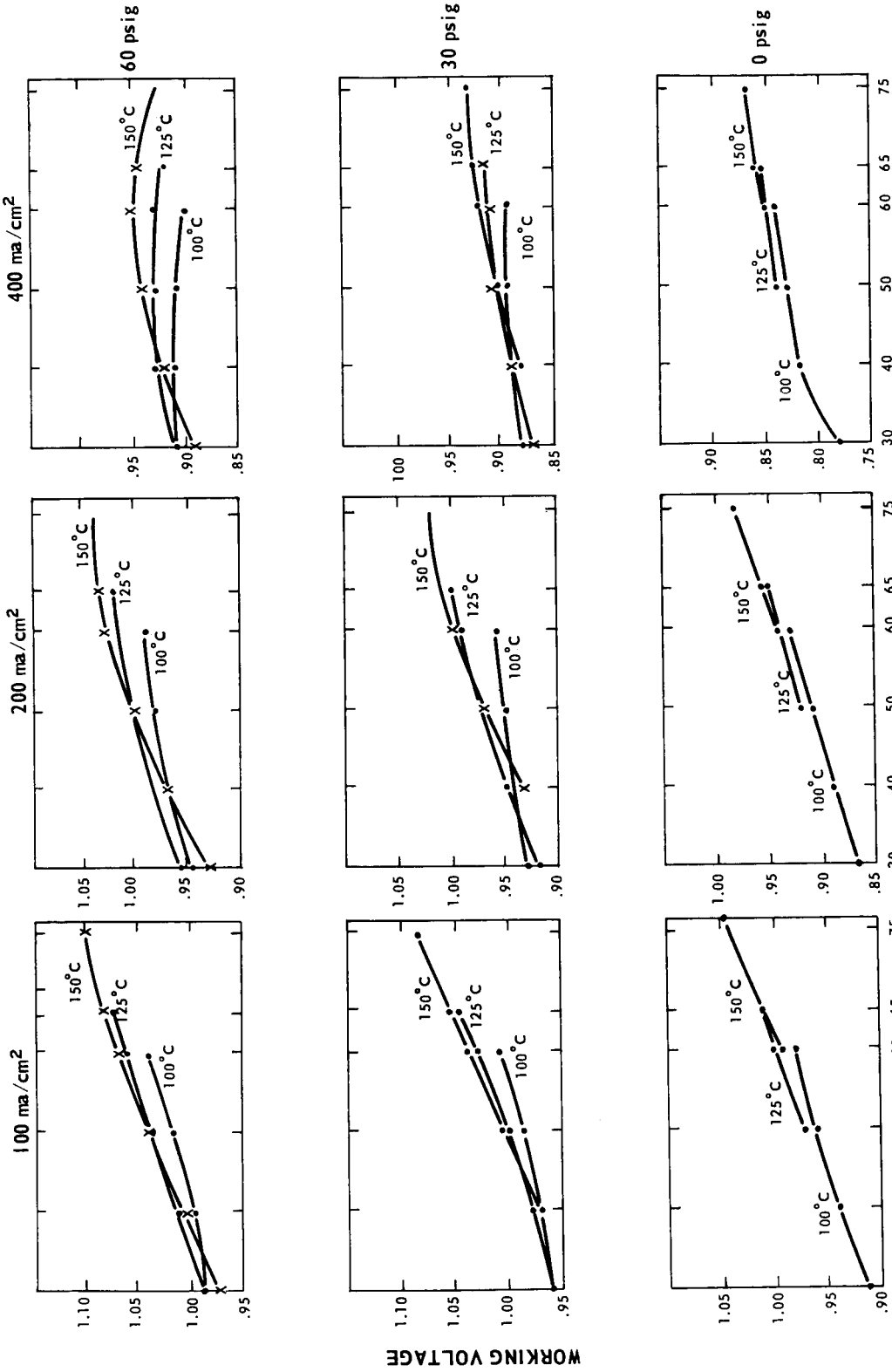
FIGURE 3-2

EMPIRICAL MODEL
PERFORMANCE vs. TEMPERATURE

WORKING VOLTAGE
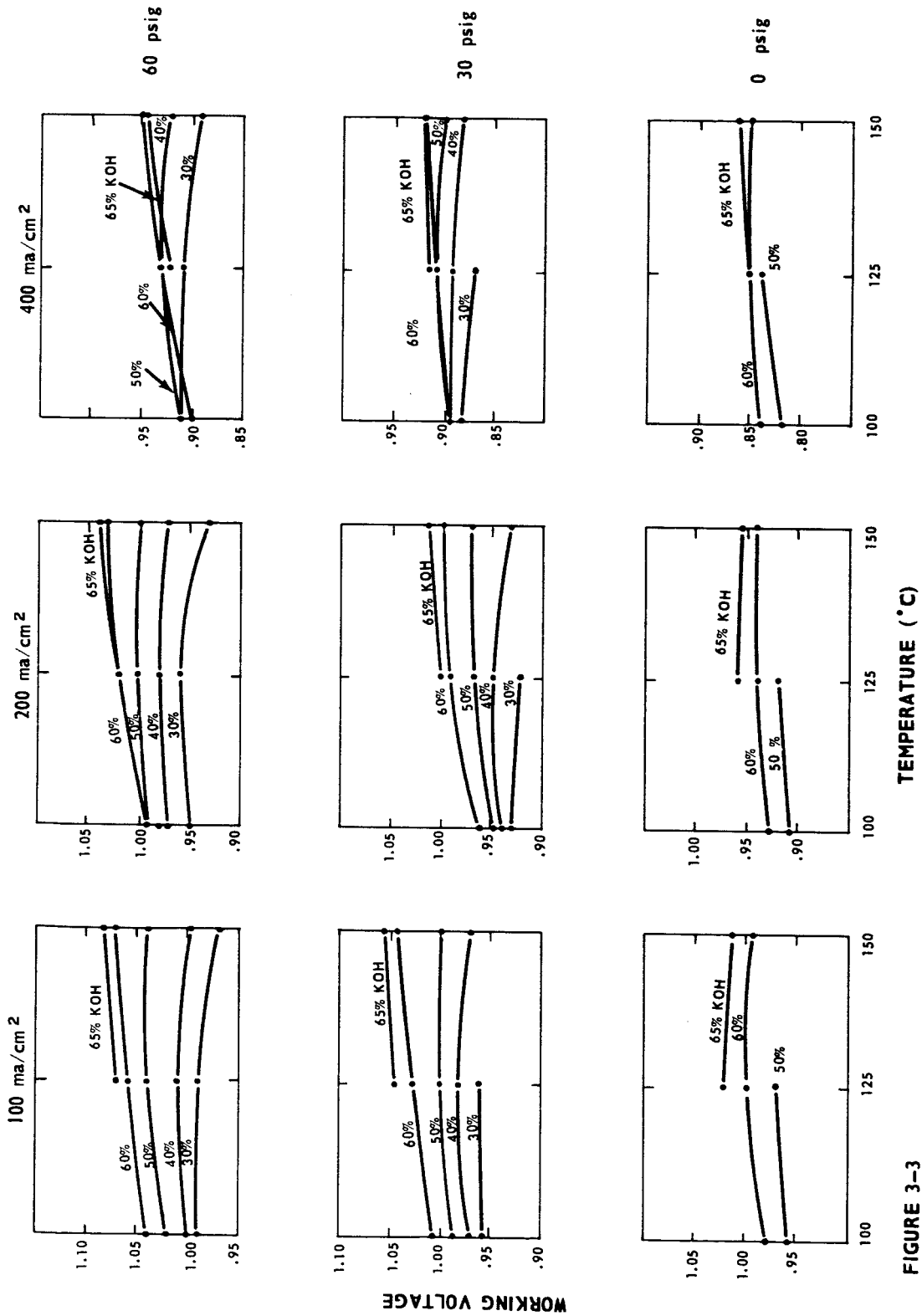
TEMPERATURE (°C)

FIGURE 3-3

3.2.3 Effects of Operating Variables

Figures 3-1, through 3-3 show also the effects of pressure, KOH concentration and temperature respectively on initial performance. These effects are qualitatively the same as were indicated previously (3) by more limited direct comparisions of the experimental data. It can be seen that the magnitude or even the direction of the effect on cell voltage caused by changes in each operating variable depends on the levels of the other variables. This is because the effects of these variables on the reversible emf, on the various polarizations (activation, gas concentration, and electrolyte concentration) and on cell resistance are interdependent. The interactions of the operating variables predicted by the empirical model can be explained qualitatively by fuel cell theory as discussed by Adams, Brown, and Watson.[4]

3.2.3.1 Pressure

Increased pressure substantially raises the voltage at all levels of the other variables (Figure 3-1). Theoretically, this results from an increase in the reversible emf, from a decrease in activation polarization, (caused by an increase in the exchange current), and from a decrease in gas concentration polarization, (resulting from increased solubility of the reactant gases in the electrolyte). Since the voltage improvement (50-130 mv) caused by an increase in pressure from 0 to 60 psig is much greater than the increase in reversible emf (30 mv), the reduction of polarization losses is a substantial part of the pressure effect.

The magnitude of the pressure effect increases with increasing current density. An increase in pressure from 0 to 60 psig increases the voltage by 50-80 mv at 100 ma/cm^2 and by 70-130 mv at 400 ma/cm^2. This is to be expected since the reduction of gas concentration polarization is more significant at higher current densities.

The magnitude of the pressure effect diminishes somewhat with increasing pressure. Nevertheless, the voltages predicted at 60 psig are significantly higher, (by 15-30 mv) than at 30 psig.

3.2.3.2 KOH Concentration

Increased KOH concentration substantially increases the voltage at nearly all levels of the other variables (Figure 3-2). The magnitude of this effect decreases with increasing current density. Thus at 100 ma/cm^2, the voltage is 50-100 mv higher at 60% KOH than at 30% KOH and increases over concentration ranges up to 5% below the solubility limit. By contrast, at 400 ma/cm^2 the voltage either increases or decreases with increasing concentration, depending on the pressure, and ranges from 10 mv lower to 60 mv higher at 60% KOH than at 30% KOH. This is to be expected qualitatively from the opposing theoretical effects of KOH concentration on cell voltage. On the one hand, an increase in concentration lowers the vapor pressure and increases the partial pressures of the reactant gases. This tends to increase cell voltage, both by raising the reversible emf and by decreasing activation polarization. However, at concentrations above those which yield minimun resistivity [30-50% KOH at 100-150°C (5)] an increase in concentration increases

cell resistance. This tends to lower cell voltage particularly at high current density. Referring again to Figure 3-2, the tendency of increasing concentration to raise cell voltage predominates at all but the highest combination of current density (400 ma/cm^2) and pressure (60 psig).

It is of interest to note that as the pressure is raised there is less voltage improvement with increasing concentration. This is probably because a given increase in KOH concentration raises the reactant partial pressures relatively less as the total pressure is increased. Thus, at $100°$C, a rise in KOH concentration from 30% to 60% raises the reactant partial pressures by 130% [from 300 mm Hg to 694 mm Hg (6)] at 0 psig but only by 11% [3420 mm Hg to 3814 mm Hg] at 60 psig (6). At 60 psig, and 400 ma/cm^2 the tendency of increasing KOH concentration to raise cell voltage is apparently diminished sufficiently so that, at concentrations above these yielding minimum resistivity, the resistive effect predominates and voltage decreases with increasing concentration.

The concentration effect increases with increasing temperature. This is to be expected because, at the resulting higher vapor pressure, a given increase in KOH concentration is relatively more effective in raising the partial pressures of the reactant gases. Furthermore, an increase in temperature lessens adverse resistive and/or diffusional effects in the electrolyte as its concentration is increased.

3.2.3.3 Temperature

In the range 100-150°C, temperature has little effect on the voltage except at concentrations approaching the solubility limits at 100-125°C, i.e., at 60-65% KOH (Figure 3-3). With these high loading electrodes the principal effect of increasing the temperature in this range is probably the reduction of polarization associated with electrolyte or gas diffusion limitations. Thus, the major advantage, for initial performance, of increasing the temperature is the possibility of operating at higher KOH concentrations (Figure 3-2).

3.2.3.4 Highest Initial Performance

Within the region of operating variables the model predicts that at all current densities the highest initial performance can be obtained at 150°C and 45-60 psig. The KOH concentrations yielding highest performance at 100, 200, 300 and 400 ma/cm^2 are 75%, 70-75%, 65-70% and 60-65%, respectively. The maximum initial voltages at these same current densities are respectively 1.10 v, 1.04 v, 0.99 v and 0.95 v. These voltages were actually obtained, within 10 mv, in the experimental runs reported previously.

These initial performances values predicted for the AB-40 electrodes are based on a matrix of 16-18 mil ACCO-II Asbestos. It is reasonable to assume that a different matrix whose resistance is close to that of ACCO-II Asbestos should give very nearly the same initial performance. It is estimated that a thinner less resistive matrix might increase the voltage by as much as 30 mv at 100 ma/cm^2 and as much as 100 mv at 400 ma/cm^2.

3.2.4 Fraction of Water Removed at Each Electrode

The effect of the fraction of water removed at each electrode on the initial performance was investigated at a condition perferred for life-testing, i.e., 100°C, 0 psig and 50% KOH. The matrix (ACCO-II Asbestos) was the same as that used to determine the effects of temperature, pressure, and KOH concentration on initial performance.

Figure 3-4 shows the effect of the fraction of water removed at the hydrogen electrode on initial voltage. The data are for second polarization curves. At current densities up to 200 ma/cm^2 the voltage increased continuously with the increasing fraction of water removed at the hydrogen electrode. With all water removed on the hydrogen side, the voltage was 40 mv higher at 100 ma/cm^2 and 30 mv higher at 200 ma/cm^2 than when all water was removed on the oxygen side. At 300-400 ma/cm^2, the voltage was approximately constant, within 20 mv, at any fraction. At 600-1000 ma/cm^2 the voltage was approximately constant in the fraction range 0-1/3 and then decreased markedly in the range 1/3-1. At 800-1000 ma/cm^2, the voltage was unstable when all water was removed at the hydrogen electrode.

3.3 Life-Testing

Life-testing in 2-inch cells is now conducted in new test facilities within the Stamford Laboratories. During the current reporting period three life tests were moved to these facilities after they had been started.

INITIAL PERFORMANCE vs. FRACTION OF WATER REMOVED AT HYDROGEN ELECTRODE

FRACTION OF PRODUCT WATER REMOVED AT HYDROGEN ELECTRODE
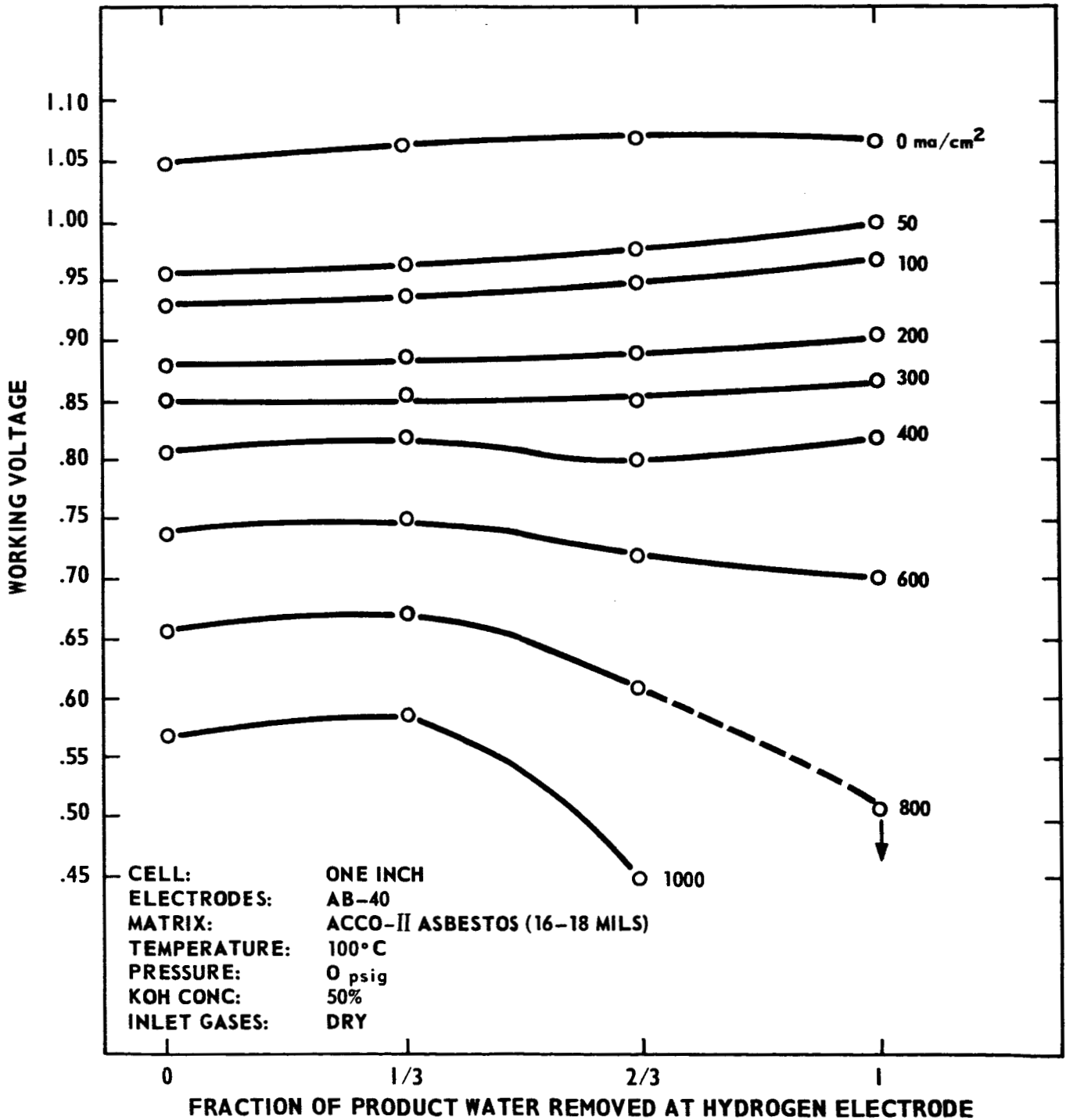
FIGURE 3–4

Life tests were run at 100°C with asbestos matrices (20-25 mils) at current densities of 100-400 ma/cm^2 and pressures of 0-15 psig. Acceptable voltage stability was achieved for more than 1200 hours at current densities up to 300 ma/cm^2. Tests were also conducted at 125°C with a PTFE-Asbestos matrix and at 150°C with porous PTFE matrices. Table 3-3 summarizes all tests. Figures 3-5 through 3-10 show the change of cell voltage and resistance with time.

3.3.1 Tests at 100°C

Life tests at 100°C and 50% KOH are discussed below in the order of increasing current density.

3.3.1.1 Tests at 100 ma/cm^2

Runs at 100 ma/cm^2 and atmospheric pressure are shown in Figure 3-5. Tests employing ACCO-I Asbestos (TLT-2-322) and Fuel Cell Asbestos (TLT-2-324) as the matrix have passed contract specifications for stable operation. Both of these tests have run at 0.92-0.94 v. for 1480 hours at a voltage decline rate of 1.7 mv/100 hours.

A test employing ACCO-II Asbestos as the matrix (TLT-2-323) ran stably for 640 hours at a voltage level of 0.90-0.92 v and a voltage decline rate of 2.5 mv/100 hours. The run was terminated by a temperature controller failure. Quinterra Asbestos has also yielded stable performance for 429 hours at 0.94 v with no decline in voltage (TLT-2-354).

The first three of the tests described above were run on humidified gases while the fourth was run on dry gases. Thus either gas condition appears suitable for stable operation at 100 ma/cm^2.

TABLE 3-?

Life Tests: 2" x 2" Cell[a]

Test no.	Matrix	Thickness (Mils)	Current Density (ma/cm²)	KOH Conc. (%)	KOH Loading (g/g Matrix)	Inlet Gas Condition	Inlet Gas Flow Rates (cc/min at 0 psig, 23°C) H₂	O₂	Inlet Flow Ratio (H₂/O₂)	Test Duration (Hours)	Working Voltage (v) Initial	Maximum	Now or Final	Overall Voltage Decline Rate (mv/100 Hours)	Cell Resistance (Milliohms) Initial	Minimum	Now or Final	Status	Reason For Termination
Tests at 100°C																			
2-322	ACCO-I Asbestos	25	100	50	3.1	Humidified at 45°C	74	74	1.0	1482	.944	.944	.919	1.7	4.2	3.4	3.7	Continuing	-
2-323	Fuel Cell Asbestos	22	"	"	1.3	"	"	"	"	1481	.915	.954	.924	"	7.1	5.8	7.6	"	-
2-321	ACCO-II Asbestos	21	"	"	3.1	"	"	"	"	641	.925	.925	.910	2.5	4.8	3.5	4.2	Terminated	(1)
2-354	Quinterra Asbestos	23	"	"	3.2	Dry	48	48	"	429	.928	.938	.934d	0	5.3	3.3	3.4	Continuing	-
2-314 b,c	ACCO-I Asbestos	25	"	"	3.1	"	51	45	1.1	187	.902	.904	.860d	25d	5.2	4.0	5.0	Terminated	(2)
2-317 e,f	ACCO-II Asbestos	20	200	50	2.0	Dry	239	119	2.0	451	.904	.923	.900d	5.5d	4.6	3.7	4.0	Continuing	(4)
2-342 e,f	Fuel Cell Asbestos	"	"	46 or 50	1.3	"	213	123	"	1098	.925	.925	.862	5.5	6.5	4.6	6.4	"	(4)
2-327	ACCO-II Asbestos	22	"	50	2.0	"	96	96	1.0	184	.904	.835	.831	-	5.5	3.2	4.0	Terminated	(4)
2-355	ACCO-I Asbestos	21	300	"	3.3	"	144	144	"	1242	.878	.884	.864	1.5	3.9	3.0	3.2	Continuing	-
2-305	"	25	"	"	3.1	"	"	"	"	1321	.876	.876	.777	7.5	5.7	3.3	4.2	Terminated	(4)
2-331	"	21	"	"	"	"	"	"	"	18	.877	.877	.776	-	5.2	3.1	3.1	"	(2)
2-329	"	24	"	"	"	"	"	"	"	137	.850	.850	.821	21	2.3	2.3	3.1	"	(2)
2-337	"	21	"	"	3.3	Humidified at 45°C H₂ Humidified O₂ Dry	222	222	"	427	.872	.876	.871d	0.5d	3.8	3.8	3.1	"	(2)
2-351	"	42	"	"	3.1	O₂ Dry	615	30+	20g	478	.857	.872	.803	13	6.2	4.8	5.0	Continuing	-
2-355h	"	20	"	"	2.0	Dry	144	144	1.0	426	.863	.884	.863	5.0	4.4	3.4	3.5	"	(4)
2-356	ACCO-II Asbestos	20	"	2.0	"	"	"	"	"	1319	.875	.861	.755	10	4.6	3.3	4.4	Terminated	(4)
	Fuel Cell Asbestos	22	"	1.3	"	"	"	"	641	.850	.853	.689	22	6.4	4.7	4.8	"	(4)	
2-347	"	20	"	"	H₂ Humidified at 45°C	222	222	"	410	.833	.847	.757	32	6.8	5.0	5.0	"	(4)	
2-35?	"	22	"	1.5	Humidified at 55°C	345	345	"	454	.804	.840	.745	20	6.6	5.3	5.6	"	(4)	
2-352	"	20	"	"	H₂ Humidified at 55°C O₂ Dry	615	30+	20g	305	.806	.830	.585	90	6.4	5.2	5.4	"	(4)	
2-297	ACCO-I Asbestos	25	4.0	"	3.1	Dry	128	256	0.5	530	.810	.842	.831j	erratic	3.5	3.1	3.4	Continuing	(3)
2-374		25	"	"	"	"	256	128	2.0	864	.783	.854	.811	11	4.6	2.8	2.8	"	-
2-370	"	25	"	"	"	Humidified at 45°C O₂ Dry	536	40+	13g	1152	.809	.885	.665	10	3.6	2.9	3.2	Terminated	(4)
2-29? k	"	25	"	"	"	Humidified at 40°C Dry	246	246	1.0	530	.683	.867	.832	7.0	6.2	2.8	3.2	"	(2)(4)
	"	25	"	"	"	"	"	"	"	0	-	-	-	-	3.8	-	-	"	(5)
2-?	"	25	"	"	"	Humidified at 40°C	"	"	"	18	.774	.774	.670	-	6.2	4.4	7.5	"	(4)
Tests at 120°C																			
2-?	ACCO-II Asbestos	20	100	60	2.8	Humidified at 55°C	160	160	1.0	336	.941	.903	.767	60	5.0	5.0	11.2	Terminated	(4)
2-?	PTFE-Asbestos	24	"	"	1.1	"	128	192	0.67	425	.922	.956	.854	24	8.5	8.5	13.5	"	(6)
Tests at 12?°C																			
2-3?	PTFE l (Uncreated)	19	100	70m	2.5	Dry	63	63	1.0	0	.236	.236	.128	-	196	52	52	Terminated	(2)
2-?	"	20	"	"	0.6	Humidified at 55°C	-	75	"	0.7	-	-	.344	-	-	-	-	"	(2)
2-?	50/50 ceria-PTFE	2?	"	65	1.4	"	75	75	"	42	.966	.990	.344	> 200	5.6	5.6	28.5	"	(4)

a. All tests use prewet AB-40 electrodes unless noted otherwise.
b. 12% PTFE in electrodes.
c. Dry electrodes.
d. Prior to voltage decline.
e. Polarization curve run prior to test.
f. Cell initially steady-ended.

h. Matrix contains 20% binder instead of the usual 10%.
i. Gases directed parallel to electrodes at cell inlet.
j. Prior to transfer of cell to new testing facility.
k. Never reached operating current density.
l. Chemplast 233 ws.
m. Surfactant FC-128 (3M Co.) used in electrolyte.

Reasons for Termination
(1) Temperature controller failed.
(2) Gas cross-leakage.
(3) Test would not re-start properly after transfer to new testing facility.
(4) Low voltage level.
(5) Test did not reach operating current density.

FIGURE 3-5

LIFE TESTS AT 100 °C.: 100 ma/cm²

PRESSURE: 0 ps.ig

TLT-322 (ACCO-I ASBESTOS)

TLT-2-324 (FUEL CELL ASBESTOS)

TLT-2-354 (QUINTERRA ASBESTOS)

324(CONT'D)

-322(CONT'D)

X—TEMPERATURE CONTROLLER FAILURE

TLT-2-323 (ACCO-II ASBESTOS)

TLT-2-314 (15% PTFE IN ELECTRODES INSTEAD OF USUAL 25%)

GAS CROSS-LEAKAGE

CELL RESISTANCE (MILLIOHMS)

-324

-322

-324(CONT'D)

-323

X

-322(CONT'D)

-354

X -314

WORKING VOLTAGE

TIME(HOURS)

FIGURE 3-6

- 32 -
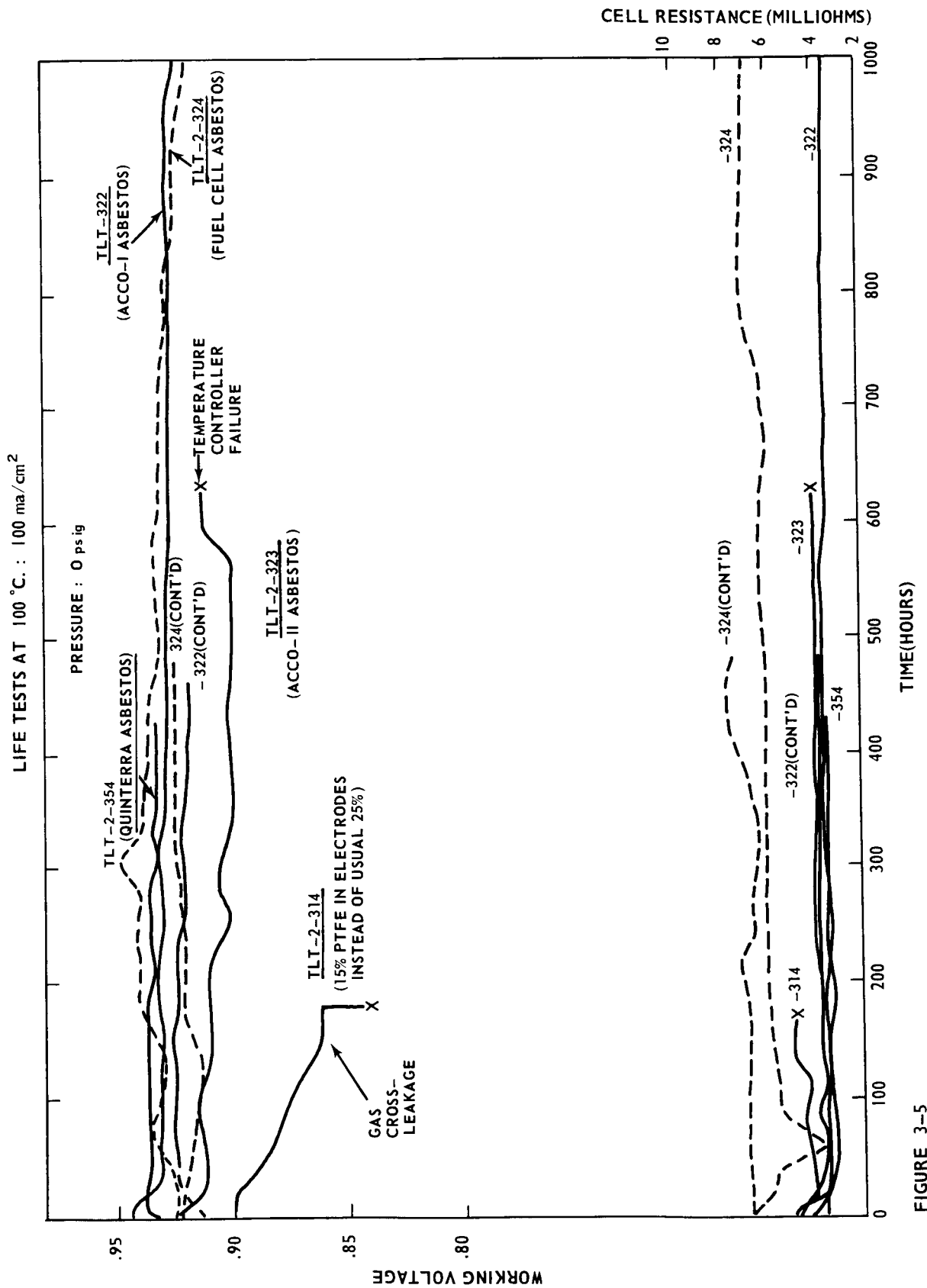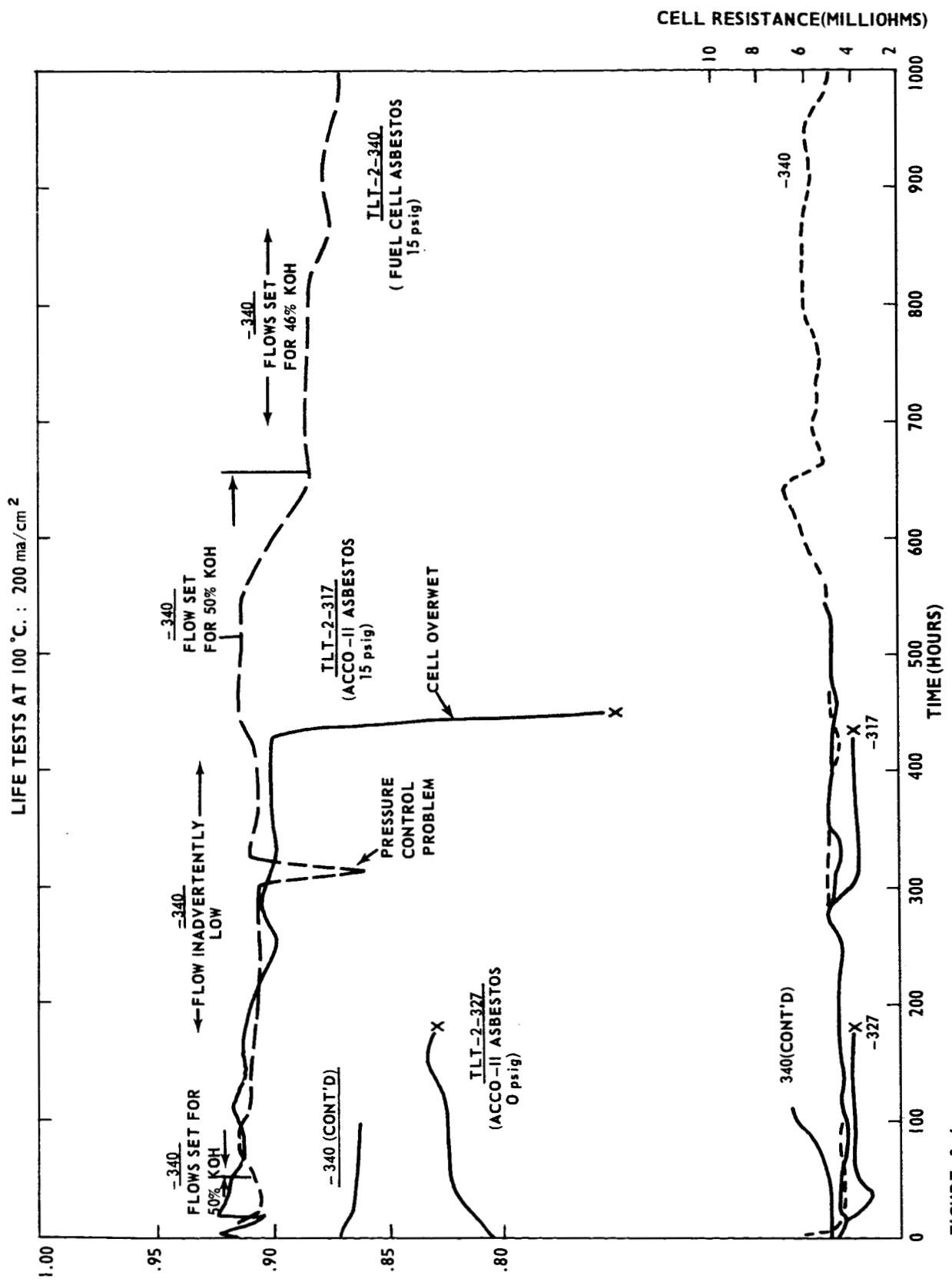
LIFE TESTS AT 100°C: 300 ma/cm²
ACCO-I ASBESTOS

PRESSURE: 0 psig

CELL RESISTANCE (MILLIOHMS)

WORKING VOLTAGE

TIME (HOURS)
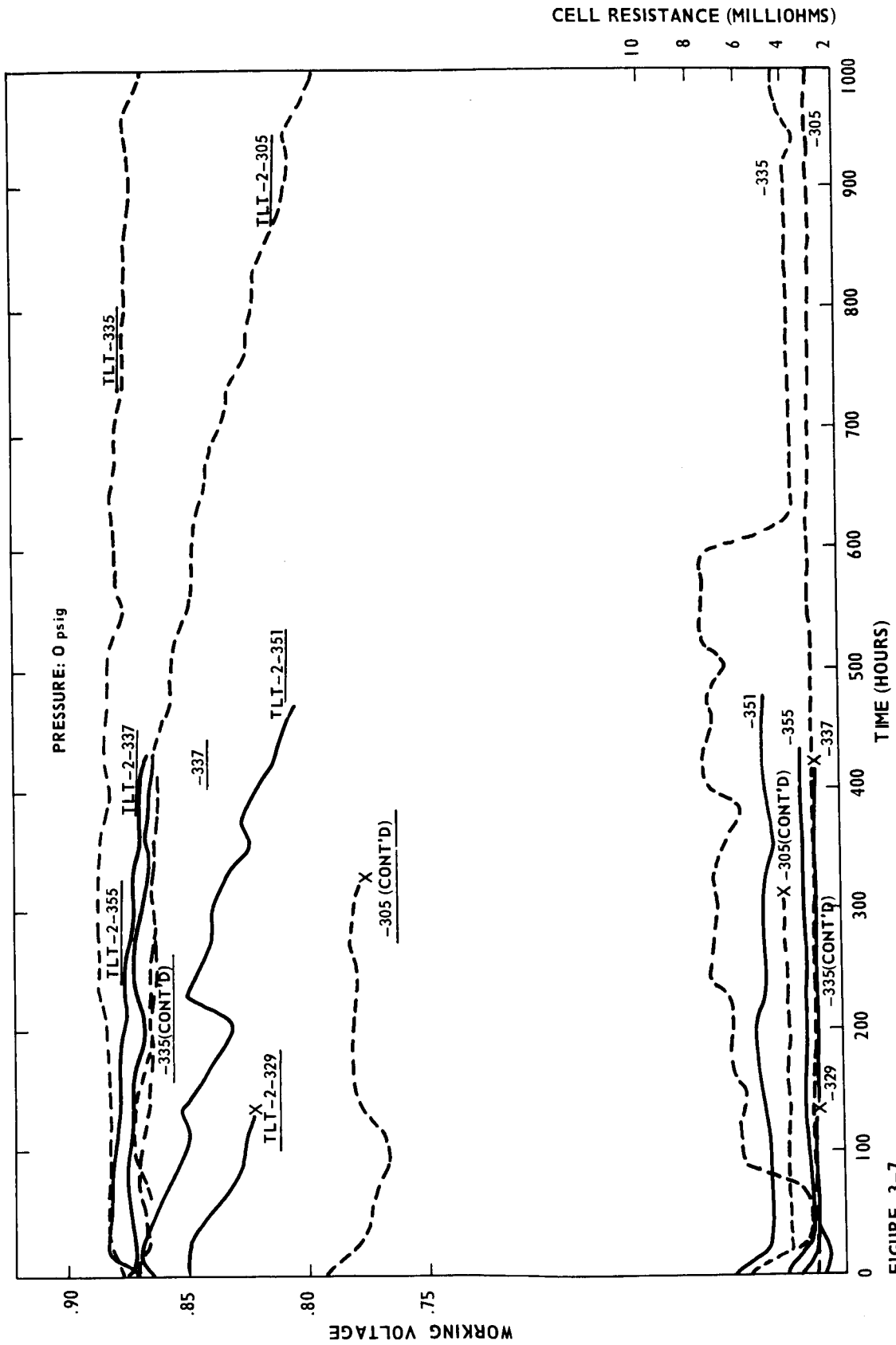
FIGURE 3-7

LIFE TESTS AT 100 °C: 300 ma/cm²
ACCO-II ASBESTOS & FUEL CELL ASBESTOS

PRESSURE: 0 psig

FIGURE 3-8

LIFE TESTS AT 100 °C. : 400 ma/cm²

MATRIX : ACCO –1 ASBESTOS
PRESSURE : 0 psig

CELL RESISTANCE (MILLIOHMS)

WORKING VOLTAGE

TIME (HOURS)

O₂ PURGE

TLT-2-298

TLT-2-297

TLT-2-303

TLT-2-304

-303(CONT'D)

-303

-303(CONT'D)

-297

-298

-303

-304

FIGURE 3-9

LIFE TESTS AT 125 °C. :

CURRENT DENSITY : 100 ma/cm^2
PRESSURE: 0 psig

FIGURE 3-10

A test was run at 100 ma/cm^2 with electrodes containing 15%
PTFE instead of the usual 25% (TLT-2-314). The matrix was ACCO-I
Asbestos. Although the cell resistance was normal and remained nearly
constant, the initial voltage (0.902 v) was low and the voltage declined
rapidly (25 mv/100 hours). The test was terminated after 187 hours
because of a cross-leakage of gas.

3.3.1.2 Tests at 200 ma/cm^2

Life tests at 200 ma/cm^2 are shown in Figure 3-6. Test
TLT-2-327 was run at atmospheric pressure with ACCO-II Asbestos as the
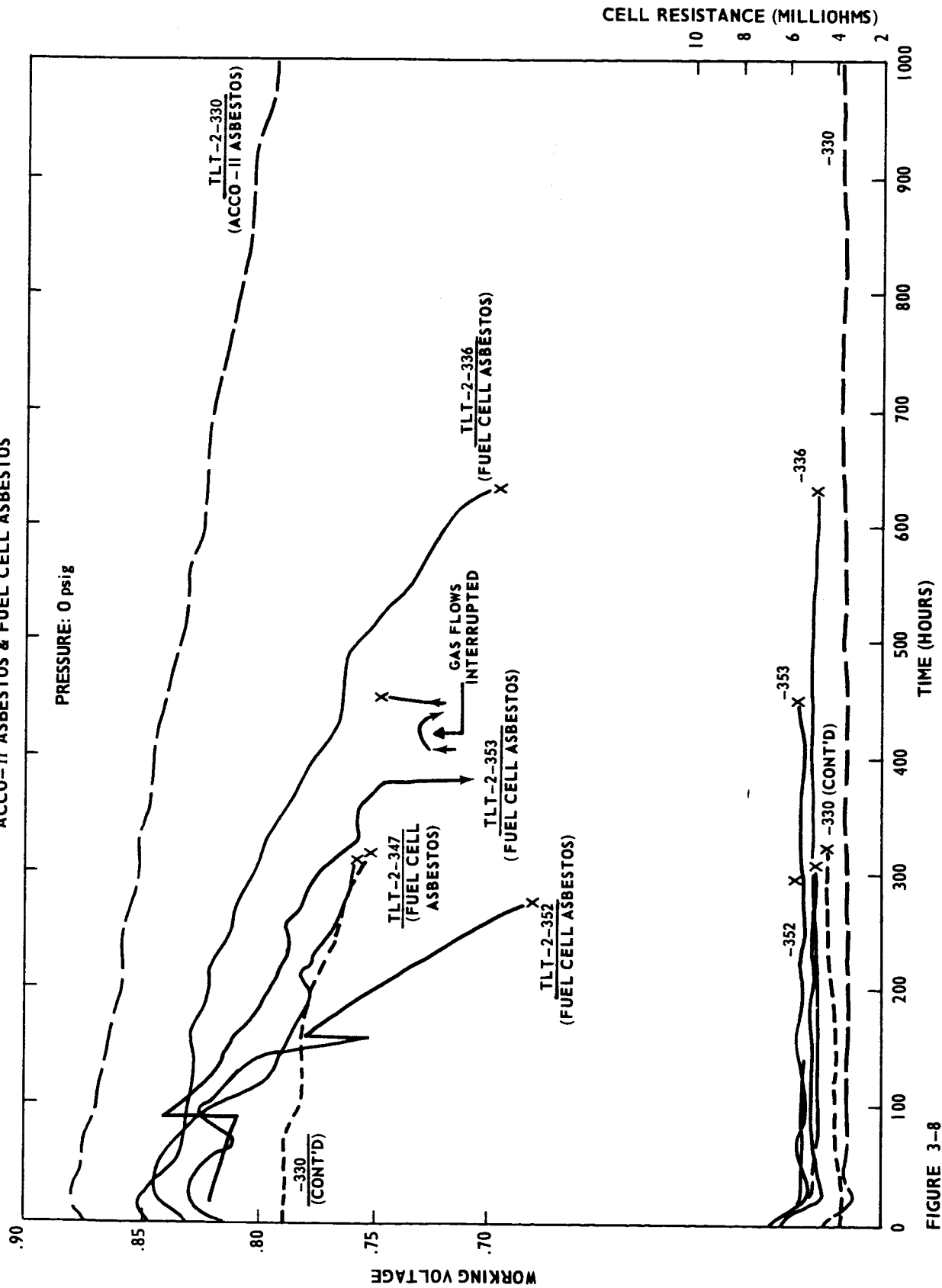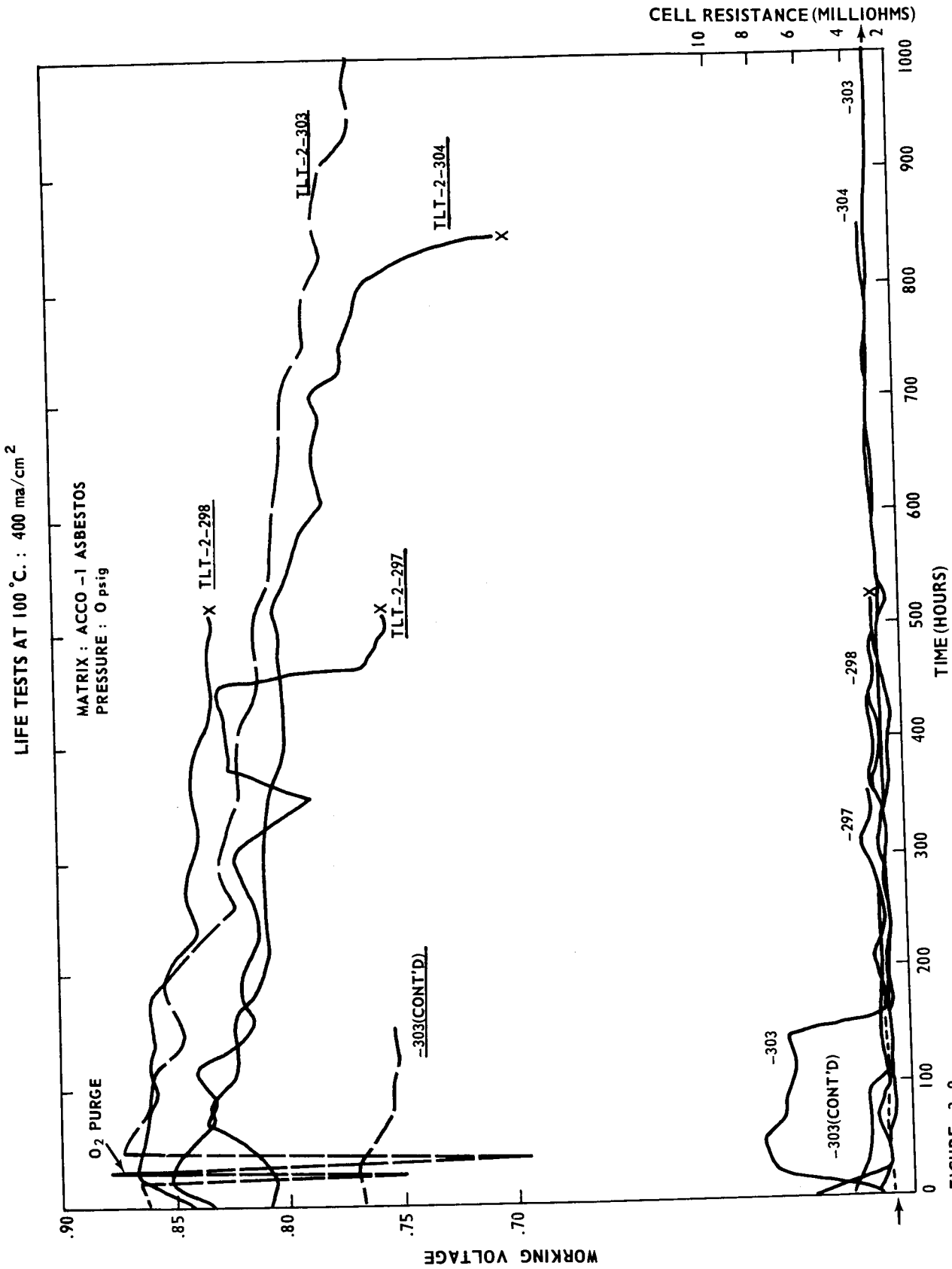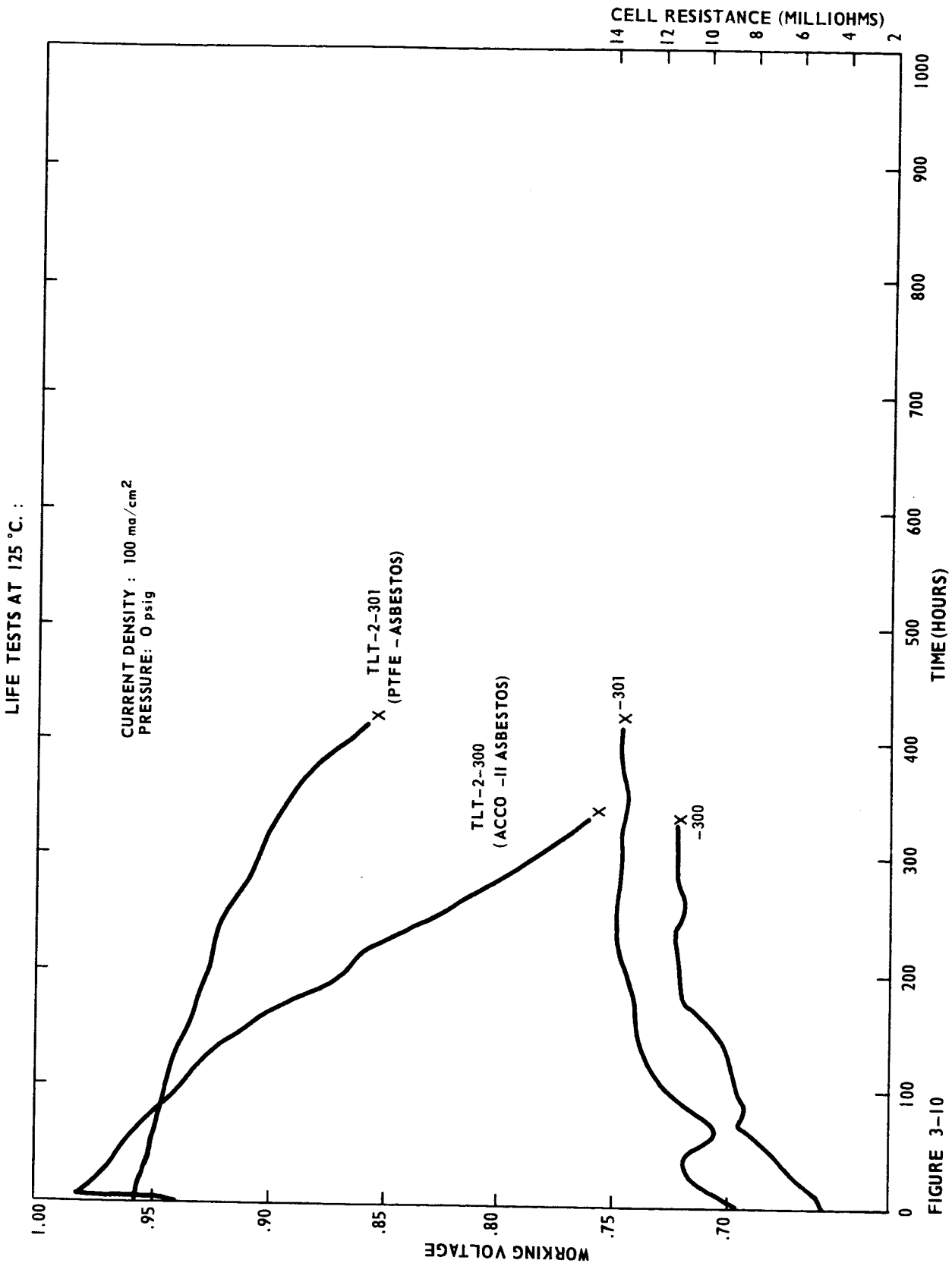matrix. The initial voltage (0.804 v) was very low and rose to a
maximum of 0.835 v during the first 160 hours. Since the maximum voltage
was still very low the run was terminated after 184 hours. The low
voltage level was probably caused by overwet electrodes (in this test
the electrodes were loaded with electrolyte to about 44% of their
weight compared to the more normal 20-30%).

Several runs were made at 200 ma/cm^2 and 15 psig on dry gases.
In a test with ACCO-II Asbestos (TLT-2-317), the initial voltage
(0.904 v) climbed to a maximum of 0.923 v during the first 24 hours.
Thereafter, the voltage decline rate was somewhat high (5.5 mv/100 hours)
although the cell resistance remained essentially constant. At 451 hours,
the voltage dropped abruptly and the run was terminated. Disassembly of
the cell revealed that the electrodes and matrix were excessively wet.

A test at 15 psig was set up with a Fuel Cell Asbestos matrix
(TLT-2-340). Initial voltage was 0.925 v. At different periods during
this test the gas flows were set to maintain either 50% or 46% KOH in

the cell. As shown in Figure 3-6, the test ran stably at 46% KOH. The voltage decline rate was zero and 4.8 mv/100 hours during separate periods of 500 hours and 450 hours respectively. However, at 50% KOH the voltage declined very rapidly, 30–85 mv/100 hours during two separate periods. The voltage decrease was accompanied by a marked rise in cell resistance indicating that local drying probably occurred at one or both of the electrodes.

3.3.1.3 Tests at 300 ma/cm^2

Figure 3-7 shows life tests at 300 ma/cm^2 with ACCO-I Asbestos. Figure 3-8 shows tests with ACCO-II Asbestos and Fuel Cell Asbestos. At this high current density, ACCO-I Asbestos gave much more stable operation than either of the other two matrices.

With ACCO-I Asbestos, test TLT-2-335 has passed contract specifications for stable operation. The test has run, on dry gases, at 0.86–0.88 v for 1242 hours at a voltage decline rate of only 1.5 mv/100 hours. This decline rate is below the lowest rate reported previously[2] for the same operating conditions (4.2 mv/100 hours for 1050 hours).

Test TLT-2-305 was run under the same conditions at TLT-2-335 except that the polarization curve was run out to 900 ma/cm^2 prior to the test. During the first 440 hours, the test ran stably at 0.86–0.87 v and a voltage decline rate of 2.5 mv/100 hours. From 440 to 1321 hours, the voltage decline rate increased to 9 mv/100 hours. The overall decline rate was 7.5 mv/100 hours.

In some runs with ACCO-I Asbestos, gas cross-leakage occurred through the matrix after some period of time. Thus tests TLT-2-331 and -329, which were run under the same conditions as TLT-2-225, developed

cross-leakage at 18 and 137 hours respectively and were terminated. Test TLT-2-337 ran with both inlet gases humidified at 45°C. During 427 hours the performance was extremely stable at 0.87 v. Cross-leakage then developed and the test was terminated.

Two tests were run with ACCO-I Asbestos under conditions substantially different from those described above. In both runs the oxygen stream was essentially dead-ended, i.e., the exit oxygen stream was a negligible fraction of the exit hydrogen stream. One test TLT-2-351) employed two 21-mil sheets of the matrix. The maximum voltage (0.872 v) was within the range usually obtained with one sheet. However, during 478 hours the voltage decline rate was high (13 mv/100 hours). The other test (TLT-2-355) employed a matrix containing 20% binder instead of the usual 10%. During 426 hours, the voltage (0.86-0.88 v) was the same as with normal ACCO-I Asbestos. The voltage decline rate (5.0 mv/100 hours) was slightly above that considered stable (4.2 mv/100 hours).

ACCO-II Asbestos (20 mils) was employed as the matrix in one test on dry gases (TLT-2-330). The initial voltage was 0.875 v. During 481 hours the voltage decline rate was high (10 mv/100 hours).

Tests with Fuel Cell Asbestos (20-22 mils) have not run stably at 300 ma/cm^2, either on dry gases or on humidified gases (TLT-2-336, -347, -352, and -353). Maximum voltages (0.83-0.85 v) were lower than the maximum voltages obtained with ACCO-I Asbestos (0.86-0.88 v). The voltage decline rate was not significantly affected by the humidity of the inlet gases. At an inlet H_2/O_2 ratio of 1.0, the voltage decline rates

where 20-32 mv/100 hours regardless of whether the inlet gases were dry or humidified at 45-55°C. The gas flow ratio appeared to have a greater effect on stability. Thus operation with the oxygen stream essentially dead-ended (inlet $H_2/O_2 = 20$) yielded a much greater voltage decline rate (90 mv/100 hours) than did an equal flow split (TLT-2-352).

3.3.1.4 Tests at 400 ma/cm^2

All tests at 400 ma/cm^2 employed <u>ACCO-I Asbestos</u> as the matrix since it alone gave stable performance at 300 ma/cm^2. In all runs the KOH loading was 3.1 g/g dry matrix. Results are shown in Figure 3-9.

Test TLT-2-297 was run on dry gases with most of the water removed at the oxygen electrode. During 460 hours the voltage fluctuated erratically, mostly in the range 0.81-0.84 v. Nevertheless at 460 hours, the voltage (0.831 v) was only 11 mv below the maximum voltage of the test. This voltage behavior indicates that no irreversible phenomenon, such as electrode deterioration, was occurring. At 460 hours the cell was transferred to the new testing facilities. The test did not restart properly and was terminated.

Test TLT-2-304 was also run on dry gases but with most of the water removed at the hydrogen electrode. To minimize the possibility of overdrying the electrode areas adjacent to the inlet gas ports, the inlet gases were made to impinge on the modified gasket before flowing parallel to the electrodes. The voltage fluctuated much less than in TLT-2-297. During 800 hours the overall voltage decline rate was 11 mv/100 hours. The decline rate then accelerated due to cross-leakage of gas and the test was terminated. However, during 320 hours (220-540

hours total elapsed time), the voltage was stable at a decline rate of only 1.2 mv/100 hours. Voltage stability for this length of time shows that even at 400 ma/cm^2 the mass transfer rates of reactant gases and product water within the cell are sufficiently rapid for stable operation with this electrode-matrix system.

Test TLT-2-303 was run with the inlet hydrogen humidified at 45°C and the oxygen essentially dead-ended. During 1340 hours the voltage decline rate was 10 mv/100 hours.

The lowest overall voltage decline rate obtained to date was 7 mv/100 hours for 530 hours (TLT-2-298). In this test both inlet gases were humidified at 40°C. The run was terminated when it failed to restart properly after it was transferred to the new test facility.

Runs were made with electrodes containing 15% PTFE instead of the normal 25% (TLT-2-312 and -313). TLT-2-312 was started with prewet electrodes but could not be brought up to the operating current density because the electrodes were flooded. TLT-2-313 had a low initial and maximum voltage (0.774 v) and a very rapid voltage decline and was terminated.

With the exception of the early part of TLT-2-303, the performance declines in the tests at 400 ma/cm^2 were not accompanied by a rise in cell resistance.

Although acceptable voltage stability has not yet been achieved at 400 ma/cm^2, it cannot be concluded that stable operation is improbable at this current density because the overall voltage decline rates obtained thus far (7-11 mv/100 hours) are not excessively high.

Furthermore, only limited combinations of inlet gas flow ratio and humidity have been employed. The stable operation demonstrated during 320 hours in TLT-2-304, offers promise that stability can be achieved for longer periods.

3.3.2 Tests at 125°C

Figure 3-10 shows tests at 125°C and 60% KOH.

Test TLT-2-300 was run with an ACCO-II Asbestos matrix at 100 ma/cm^2. The inlet gases were humidified. As in previous tests[2,3] with asbestos matrices at 125°C, the voltage declined very rapidly (60 mv/100 hours during 336 hours). Test TLT-2-301 employed a PTFE-Asbestos matrix and was run under the same conditions at TLT-2-300. The voltage declined at an accelerated rate during 425 hours.

In both tests the voltage declines were accompanied by a steady rise in cell resistance. This has been observed in all previous tests with asbestos-containing matrices at 125°C, though not in general at 100°C, and is probably caused by slow corrosion of the matrix in KOH.

3.3.3 Tests at 150°C

Two runs were started at 150°C and 70% KOH with 20-mil unetched porous PTFE (Chemplast 233 WS) as the matrix. The KOH contained 0.015% of FC-128 (3M Co.) as a wetting agent for the PTFE. One test (TLT-2-321) was run on dry gases while the other (TLT-2-320) was run on gases humidified at 55°C. Both tests immediately developed cross-leakage of gas and were terminated.

Test TLT-2-350 employed a 95/5 ceria-PTFE matrix at 150°C and 65% KOH. The matrix (35 mils) was thicker than those used in initial performance and short term tests (Section 3.1.1). Dew point measurements taken at 25 hours of operation showed the KOH concentration at the hydrogen and oxygen exit to be 63.5% and 66.0% respectively. During 42 hours of operation, the cell resistance increased 5-fold and the voltage decline rate was severe (>200 mv/100 hours). Additional tests with thinner ceria-PTFE matrices are planned.

3.3.4 KOH Loading and Voltage Stability

The dependence of life test stability on KOH loading is of interest. In nearly all tests, the electrodes, as well as the matrix, were loaded with 50% KOH. The electrodes were vacuum immersed in the electrolyte for one to three minutes and then blotted to obtain the desired loading. Table 3-4 gives the matrix and electrode loadings and the total loading for most of the tests run with asbestos matrices during this period. The stability of each test is also listed.

The KOH loading into the electrodes was normally 18-26% of the dry electrode weight and was evenly distributed between anode and cathode. In most runs the electrode KOH was 35-50% of the total KOH loaded into the cell, which was 4-8 grams. If the cellwere assembled with dry electrodes, the maximum amount of KOH that could be loaded via the 20-25 mil matrix alone would be approximately 6 grams.

With each type of matrix, the runs shown in Table 3-4 were made at various combinations of current density, gas flow ratio, and gas humidity which do not permit the dependence of performance stability

TABLE 3-4

KOH Loading and Voltage Stability

TLT No.	Matrix	Current Density (ma/cm²)	KOH Loading (g) Matrix	KOH Loading (g) Electrodes H₂	KOH Loading (g) Electrodes O₂	KOH in Electrodes (% of Dry Electrodes) H₂	KOH in Electrodes (% of Dry Electrodes) O₂	Total KOH Loading (g)	Overall Voltage Decline Rate (mv/100 Hrs.)	Stability
2-322	ACCO-I Asbestos	100	3.48	1.84	1.79	33.2	30.8	7.11	1.7	Stable
2-337	"	300	3.68	1.23	1.34	22.3	23.7	6.25	0.5	Stable
2-335	"	"	3.50	1.39	1.31	24.5	22.2	6.21	1.5	Stable
2-329	"	"	3.30	1.32	1.32	24.0	23.7	5.95	21	Unstable
2-331	"	"	3.50	1.09	1.01	20.4	18.6	5.60	-	Unstable (Cross-Leakage)
2-355	"	"	2.98	1.00	1.00	18.8	18.7	4.98	5.0	Nearly Stable
2-323	ACCO-II Asbestos	100	5.80	1.45	1.49	26.9	27.1	8.74	2.5	Stable
2-327	"	200	3.86	2.46	2.41	45.3	43.7	8.72	-	Low, Rising Voltage
2-317	"	"	5.24	1.12	1.03	20.4	19.2	7.40	5.5	Nearly Stable
2-328	"	300	2.74	1.26	1.27	23.6	23.4	5.28	-	Low, Rising Voltage
2-330	"	"	2.87	0.96	0.97	17.6	17.8	4.81	10	Unstable
2-324	Fuel Cell Asbestos	100	3.05	1.49	1.52	26.3	26.3	6.05	1.7	Stable
2-340	"	200	4.53	0.97	1.28	18.2	22.4	6.79	5.5	Nearly Stable
2-336	"	300	3.04	1.14	1.03	20.8	18.7	5.22	22	Unstable
2-347	"	"	2.60	1.04	1.00	19.5	18.6	4.64	32	Unstable
2-352	"	"	2.32	1.00	1.00	18.4	18.2	4.33	90	Unstable
2-353	"	"	2.26	0.99	1.03	18.7	19.3	4.28	20	Unstable
2-354	Quinterra Asbestos	100	4.77	0.98	1.00	18.7	18.6	6.77	0	Stable

on KOH loading to be determined directly. Nevertheless, stable operation appears to have occurred more frequently in the higher ranges of total KOH loading. Thus, eight of the nine tests which had a total KOH loading above six grams (6.05-8.74 g) have run stably or nearly stably at 100-300 ma/cm^2 for 427-1482 hours (TLT-2-322, -337, -335, -323, -317, -340, -324, and -354). The ninth test (TLT-2-327) ran with a low, rising voltage. By contrast, seven of nine tests which had a total KOH loading below six grams (4.28-5.45 g) were unstable (TLT-2-329, -331, -330, -336, -347, -352, and -353). One test (TLT-2-355) was stable. The ninth test (TLT-2-328) had a low, rising voltage.

The data indicate that total KOH loadings of 6-8 grams or perhaps higher are suitable for stable operation with ACCO-I Asbestos at current densities up to at least 300 ma/cm^2. The data are not sufficient to conclude whether lower loadings are unsuitable for ACCO-I Asbestos since two tests at lower loadings were unstable (TLT-2-329 and -331) while one (TLT-2-355) was nearly stable.

Total loadings above six grams appear to be suitable also for stable operation with ACCO-II Asbestos, Fuel Cell Asbestos and Quinterra Asbestos at 100-200 ma/cm^2. Lower loadings were not employed. Tests with ACCO-II Asbestos and Fuel Cell Asbestos at 300 ma/cm^2 have not run stably at loadings below six grams. Higher loadings have not yet been investigated.

3.3.5 KOH Concentration Gradient and Voltage Stability

During life testing, KOH concentration gradients develop within the matrix and electrodes. An "overall" concentration gradient extends diagonally through the matrix from the hydrogen exit at one end of the cell to the oxygen exit at the other end. The effect of this gradient on long term stability and its dependence on operating variables are of interest.

The magnitude of the overall KOH concentration gradient was determined in some runs at 100°C which employed various types of asbestos matrices of equal thickness (20-25 mils). All of these runs used the same inlet H_2/O_2 ratio (1.0) at gas rates set to maintain 50% KOH in the cell. The current density ranged from 100-300 ma/cm^2 and the inlet gases were either dry or humidified at 45°C.

The KOH concentration at each gas exit was determined from the humidity of the exit gas stream by assuming water vapor equilibrium between electrolyte and gas. The humidity was measured either by removing water from the gas in a Drierite tube for 1 1/2-4 hours or from a dew point measurement. The KOH concentrations determined from these separate measurements generally agreed within 3 wt. %.

Table 3-5 compares KOH concentration gradients with overall voltage decline rates. The concentrations, determined from water collection measurements, were in the range 42.5-50.5% at the hydrogen exit and 50.5-57.5% at the oxygen exit. The overall concentration gradient ranged from 0.5-15% KOH. In some runs concentrations were

TABLE 3-5

KOH Concentration Gradient and Voltage Stability[a,b]

Cell: Two-Inch
Electrodes: AB-40
Temperature: 100°C
Inlet H_2/O_2 Ratio: 1.0
Matrix Thickness: 20-25 Mils

TLT No.	Matrix	Inlet Gas Condition	Current Density (ma/cm²)	Overall Voltage Decline Rate[c] (mv/100 Hrs.)	Total Elapsed Time (Hrs.)	Equilibrium KOH Conc. (%) At H₂ Exit	Equilibrium KOH Conc. (%) At O₂ Exit	KOH Conc. Gradient (%)	% of Product Water Collected
2-335	ACCO-I Asbestos	Dry	300	1.5	93	45.5	52.5	7.0	102.
					260	47.5	52.5	5.0	99.8
					452	47.5	52.5	5.0	99.4
					624	46.5	51.5	5.0	100.0
					787	46.5	52.	5.5	100.0
					910	47.	51.	4.0	100.0
					978	47.	50.5	3.0	101.0
2-305	ACCO-I Asbestos	Dry	300	7.5	830	46.5	54.	7.5	99.5
					950	46.5	53.5	7.0	104
2-330	ACCO-II Asbestos	Dry	300	10	19	45.5	53.	7.5	102
					44	45.5	53.	7.5	101
					164	45.5	53.5	8.0	101
					330	45.	54.5	9.5	101
					503	45.5	55.	9.5	99.5
					695	45.	54.5	9.5	99
					858	44.5	54.5	10.0	100.5
					980	45.	53.5	8.5	100
					1051	44.	54.5	9.5	101
2-336	Fuel Cell Asbestos	Dry	300	22	165	44.5	53.5	9.0	101
					257	42.5	57.5	15.0	105.8
					428	43.5	56.5	13.0	102
					621	45.5	54.5	9.0	100
2-322	ACCO-I Asbestos	Humidified at 45°C	100	1.7	576	50.5	52.	1.5	111
					742	49.	50.	1.0	107
2-323	ACCO-II Asbestos	Humidified at 45°C	100	2.5	575	50.	50.5	0.5	88
2-324	Fuel Cell Asbestos	Humidified at 45°C	100	1.7	574	47.	50.	3.0	126.5
					741	47.5	50.	2.5	111
2-337	ACCO-I Asbestos	Humidified at 45°C	300	0.5	217	48.	51.	3.0	94
2-347	Fuel Cell Asbestos	Humidified at 45°C	300	32	50	45.	53.5	8.5	111

(a) Gas flow rates set to maintain 50% KOH in cell

(b) Data obtained by collecting water from cell exit gases for 1 1/2 - 4 hours

(c) During total elapsed time shown in Table 3-3

determined at more than one time. In all of those runs but one, the concentration gradient did not change by more than 2-3% KOH during most of the operating period.

The concentration gradient increased with increasing current density, less so with ACCO-I Asbestos than with Fuel Cell Asbestos. With ACCO-I Asbestos, the gradient increased from 1.0-1.5% at 100 ma/cm^2 to 3.0% at 300 ma/cm^2 (TLT-2-322 and -337). With Fuel Cell Asbestos the gradient was 2.5-3.0% at 100 ma/cm^2 and 8.5% at 300 ma/cm^2 (TLT-2-324 and -347).

At a given current density and inlet gas humidity, the concentration gradient increased with increasing matrix density in the order ACCO-I Asbestos, ACCO-II Asbestos, and Fuel Cell Asbestos. The increase was more marked at higher current density. Thus, at 100 ma/cm^2, with humidified gases, the gradient was slightly higher with Fuel Cell Asbestos (2.5-3.0%) than with the less dense ACCO-I and ACCO-II Asbestos (0.5-1.5%) (TLT-2-324-323 and -322). At 300 ma/cm^2 with humidified gases the gradient increased from 3.0% with ACCO-I Asbestos to 8.5% with Fuel Cell Asbestos (TLT-2-335, -305, -330 and -336). Likewise, at 300 ma/cm^2 with dry gases, the gradient was 3.0-7.5% with ACCO-I Asbestos, 7.5-10.0% with ACCO-II Asbestos and 9.0-15.0% with Fuel Cell Asbestos (TLT-2-337 and -347).

Humidification of both inlet gases at 45°C reduced the KOH concentration gradient at 300 ma/cm^2. With ACCO-I Asbestos the decrease was from (3.0-7.5%) to 3.0% (TLT-2-335, -305 and -337). With Fuel Cell Asbestos this decrease was from 9.0%-15.0%) to 8.5% (TLT-2-336, and -347).

Long term performance was stable at 100-300 ma/cm^2 when the overall KOH concentration gradient was low. Thus, of the nine tests shown, the five whose gradients were mostly below 6-7% KOH ran stably at voltage decline rates of 0.5-2.5 mv/100 hours for periods of 427-1482 hours, (TLT-2-335, -322, -323, -324, -337). By contrast the four tests whose concentration gradients were 7-15% ran unstably at voltage decline rates of 7.5-32 mv/100 hours, (TLT-2-305, -330, -336, -347).

The data help to explain why ACCO-I Asbestos has given stable operation at 300 ma/cm^2 while ACCO-II and Fuel Cell Asbestos thus far have not. The results indicate that stable operation might be achieved at 300 ma/cm^2 with ACCO-II or Fuel Cell Asbestos if the overall concentration gradient can be reduced to the low levels attained with ACCO-I Asbestos.

3.3.6 Water Balance

Cell water balance data, obtained from water collection measurements, are shown in Table 3-5. The percentage of cell product water removed by the exit gas streams was generally 99-101 for the tests run with dry gases. Two slightly higher percentages (104 and 106) were also determined. With humidified gases this percentage (88-126) appears to be more widely scattered. However, the additional factor of water entering the cell makes the determination less accurate than for dry gases.

4. LARGE CELL TESTING

Acceptable voltage stability of 6" x 6" electrodes at a current density of 300 ma/cm^2 was obtained at 100°C (Run 7556-153) for a period of 740 hours. The run was made in the flat-plate cell with 20 mil ACCO-1 asbestos as the matrix. The KOH concentration was 50% and the pressure, 0 psig. The removal of product water simulated that of a battery system with a recycle hydrogen system and dead-ended oxygen. Both the hydrogen and oxygen inlet streams were first passed through Drierite to remove water and then through Ascarite to remove as much trace CO_2 as possible. The hydrogen stream was then sparged through a water saturator at 55°C. In principle this insured that at any point on the hydrogen side of the cell the KOH concentration did not exceed 55%, i.e., was at least 10% below the solubility limit. During most of the run the oxygen entered the cell dry and while not actually dead-ended, removed only 1% of the product-water. The electrodes were prewet. The run was started at 300 ma/cm^2 without first running a polarization curve out to 1000 ma/cm^2. Thus the 10-20 mv enhancement in voltage at 300 ma/cm^2 usually associated with this procedure was not obtained.

The time history of the test is shown in Figure 4-1. The initial voltage was 0.863 v. The voltage rose to a maximum of 0.879 v within two hours and then returned to 0.863 v within the next 50 hours. During the next 380 hours the voltage was stable within the limits 0.857-0.867 v. Cell resistance was essentially constant in the range 0.6-0.7 milliohms. At a total elapsed time of 430 hours, the Ascarite tubes were replaced by fresh ones. The resulting 30-second interruption in each gas flow increased the voltage to 0.886 v with no change in cell

LIFE TEST IN 6" x 6" CELL AT 100 °C AND 300 ma/cm²

ELECTRODES: AB-40
PRESSURE: 0 psig
KOH CONC. 50%
99-100% OF PRODUCT WATER REMOVED BY HYDROGEN
HUMIDIZIED AT 55° C.

O₂ SATURATOR ON: O₂ OFF
30 SEC.

H₂ SATURATOR
TEMP. TOO HIGH

DRY O₂ AT
HIGH FLOW RATE

REPLACED ASCARITE
TUBES-GASES OFF
1 MIN.

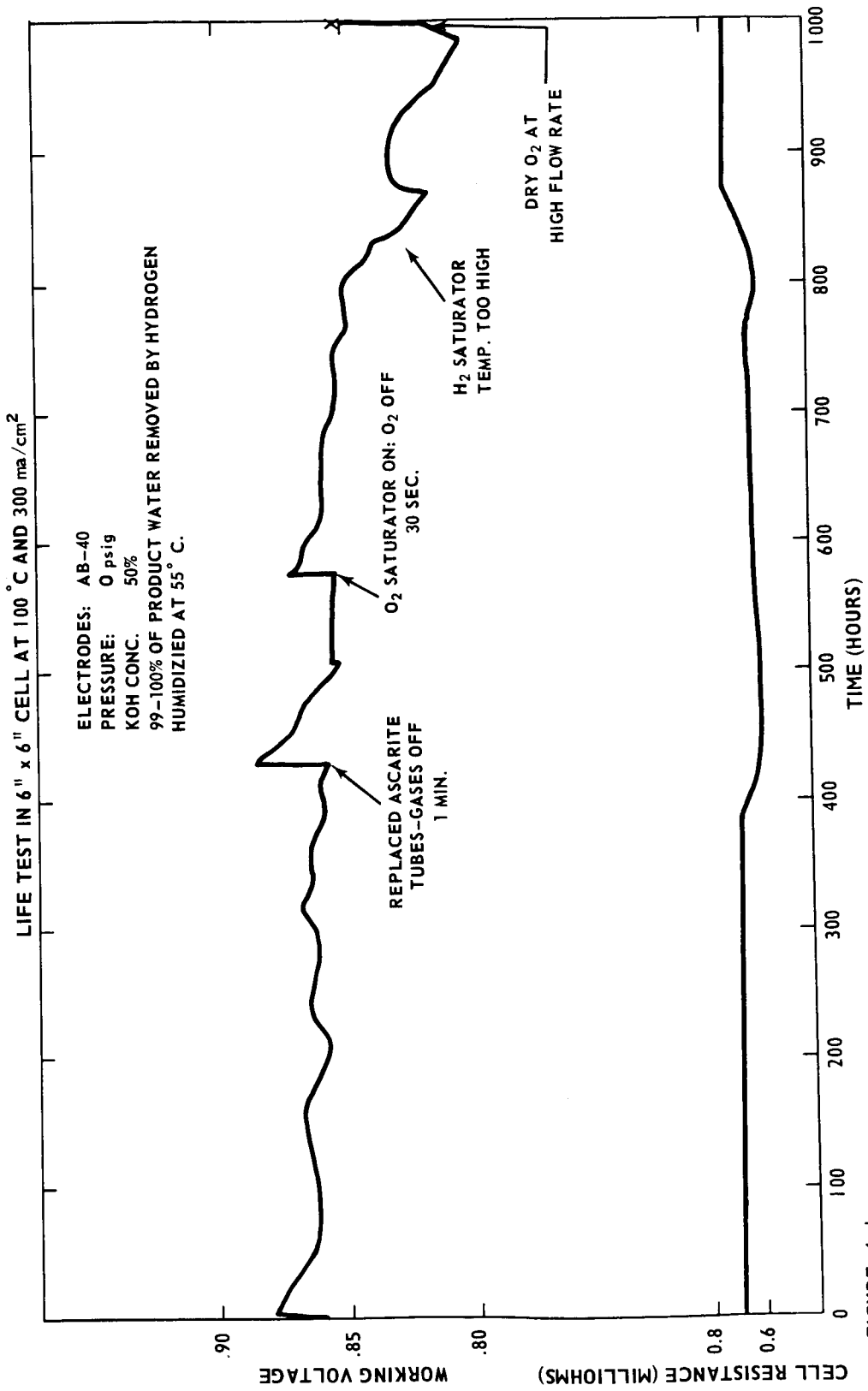TIME (HOURS)

WORKING VOLTAGE

CELL RESISTANCE (MILLIOHMS)

FIGURE 4-1

resistance. This voltage boost was dissipated during the next 70 hours. During the following 75 hours, the voltage declined slightly from 0.857 to 0.853 v. At this point the amount of product-water removed from the oxygen side was reduced from 1% of the total to zero by sparging the oxygen through water at 23-24°C. The momentary interruption in oxygen flow increased the voltage to 0.871 v. One hundred and sixty hours later the voltage was 0.854 v. Thus, after a total elapsed time of 740 hours the voltage was 9 mv below the initial voltage and the overall decline rate was 1.2 mv/100 hours.

This overall decline rate was considerably lower than that of a previous run (7556-23), at 300 ma/cm^2 (10 mv/100 hours). This appears to bear out indication from Run 7556-23 that a higher inlet hydrogen humidity and a decrease in the already small amount of water removed on the oxygen side improves long term stability. Scrubbing of both gas streams through Ascarite is another possible factor, since this had not been done in Run 7556-23.

From 740-800 hours the voltage decreased from 0.854 v to 0.848 v. From 800-850 hours the voltage declined rapidly to 0.816 v. The cause was found to be wetting of the cell due to an inadvertent rise in the temperature of the hydrogen saturator from 55°C to 61°C. The temperature rise was not readily apparent because of a faulty thermocouple. Restoration of the original saturator temperature increased the voltage to 0.832 v for 24 hours. The voltage declined to 0.803 v at 984 hours and then rose to 0.814 v at 1000 hours. Thus, the performance did not recover completely from the effect of overwetting. Water balance measurements made at 1000 hours showed that the oxygen electrode was over-wet, i.e., the KOH concentration at the oxygen exit was 40%.

The concentration at the hydrogen exit was 50%. In order to dry out the oxygen side, the oxygen was then fed dry and at an exit rate (90 cc/min) three times that used during the test. Within 15 minutes the voltage rose to 0.851 v. This confirmed that the decline in voltage after 740 hours was not caused by any cross-leakage of gas. The run was then terminated.

Inspection of the electrodes showed no serious erosion of platinum despite the high hydrogen flow rate. The matrix adhered very strongly to the hydrogen electrode but hardly at all to the oxygen electrode. Small amounts of the matrix had penetrated through the hydrogen electrode. This may have contributed to the voltage decline toward the end of the test. The gold-plated spacer-screens were only slightly discolored. The hydrogen spacer-screens contained some solid electrolyte. In each face plate, approximately 15% of the inlet gas ports contained some solid electrolyte. The oxygen face plate was highly discolored.

Despite the decline in voltage after 740 hours the total voltage decline (49 mv) during 1000 hours passed contract specifications for stable operation.

5. **FUTURE WORK**

Work for the next quarter is planned for the following tasks:

1. Corrosion data will be obtained on asbestos matrices in KOH at 100°C and on the ceria-PTFE matrix at 150°C.

2. Small Cell Life-Testing

Life tests at atmospheric pressure which are running stably will be continued beyond 1200 hours. Additional tests will be started at 100°C and 100-300 ma/cm^2 with asbestos matrices and at 125°C with the ceria-PTFE matrix.

Work on four test stations for testing at pressures above atmospheric will be completed. Runs will be made with Fuel Cell Asbestos and Quinterra Asbestos as the matrix at 100°C, 45 psig and 100-200 ma/cm^2 and with the ceria-PTFE matrix at 125°C, 45 psig and 100 ma/cm^2.

3. Large Cell Testing

Work on three test stations for life-testing under pressure will be completed. Runs will be made at 100°C, 45 psig and 100 ma/cm^2 with Fuel Cell Asbestos and Quinterra Asbestos matrices.

6. REFERENCES

(1) "Research and Development of High-Performance, Light-Weight Fuel Cell Electrodes," American Cyanamid Company, Final Report, November 1, 1963 - October 31, 1964, NASA CR-54436.

(2) "Development of High-Performance, Light-Weight Electrodes for Hydrogen-Oxygen Fuel Cells," American Cyanamid Company, First Quarterly Report, April 5, 1965 to July 5, 1965, NASA CR-54759.

(3) "Development of High-Performance, Light-Weight Electrodes for Hydrogen-Oxygen Fuel Cells," American Cyanamid Company, Second Quarterly Report, July 6, 1965 to October 5, 1965, NASA CR-54866.

(4) A. M. Adams, F. T. Brown, and R. G. H. Watson in "Fuel Cells," (W. Mitchell, Jr., ed.) Chap. 4 (Interscience) 1963.

(5) M. A. Klechko and M. M. Godneva, Zhur. Neorg Khim. (Russian) $\underline{4}$, 2130 (1959).

(6) International Critical Tables $\underline{3}$, 373.

APPENDIX

Table I

Coefficients for Direct Voltage Model

Coefficient	Value at Current Density (ma/cm^2)of:	
	100-400	600-1000
bo	+.99744	+1.01105
b1	+.0302865	+.03074413
b2	+.0107624	-.00507731
b3	-.043623	-.03280379
b4	+.0021475	+.01075729
b11	-.0013042	-.00631107
b22	-.00096667	-.01060957
b33	+.0028557	+.00035017
b44	-.00826528	+.00777593
b12	+.00058248	-.01234951
b13	-.00353551	-.00907805
b14	+.00422449	+.01879616
b23	+.00132027	+.00047435
b24	-.00166760	+.01762623
b34	+.00201633	-.00429909
b111	-.00057633	+.00431485
b222	+.00126371	+.00206583
b112	-.00187054	-.00049768
b114	+.00114904	-.02689053
b221	-.00052154	-.00048642
b224	+.00058912	+.00203244
b331	-.00043117	+.00021091

APPENDIX

Table I

(Continued)

Coefficient	Value at Current Density (ma/cm^2) of:	
	100–400	600–1000
b332	-.00009747	+.00018620
b334	-.00060917	+.00034803
b441	-.00097832	+.040607966
b442	-.00781642	+.00419566
b124	+.00314040	+.00440642

APPENDIX

Table II

Coefficients for Voltage Equation of

Indirect Voltage Model

Coefficient	Value at Current Density (ma/cm^2) of:	
	100–400	600–1000
bo	+.96750544	+1.043405
bl	+.01126123	+.01487750
b2	+.00955555	+.00579421
b3	-.02711128	-.03838096
b4	+.01756144	+.01201149
b5	+2.0832716	+4.0290962
b11	-.0018021	-.02069174
b22	-.00056277	-.00717420
b33	+.00224946	+.00062264
b44	-.01112594	-.02294152
b55	-39.051482	-156.40740
b12	-.00055880	-.01210135
b13	-.00054461	+.00172176
b14	+.01173480	+.05466973
b15	+.51738353	+3.1999481
b23	+.00201277	+.00236154
b24	+.00173633	+.02502215
b25	+.06483256	+.69047886
b34	+.0058723	-.01222065
b35	-.61928454	-1.3754686
b45	-.66520308	-4.4374492

APPENDIX

Table III

Coefficients for Resistance Equation of

Indirect Voltage Model

Coefficient	Value
d_0	+.01833
d_1	+.00124824
d_2	-.00130640
d_3	-.00086126
d_{11}	+.00295805
d_{22}	+.00130213
d_{33}	+.00084710
d_{12}	+.00171394
d_{13}	-.00225834
d_{23}	-.00108334

QUARTERLY DISTRIBUTION LIST

One copy is to be sent to each addressee, unless otherwise indicated.
Note that more than one addressee may be shown for the same address.

National Aeronautics & Space Administration
Washington, D.C. 20546
Attention: Ernst M. Cohn, Code RNW
            George F. Esenwein, Code MAT
            J. R. Miles, Code SL
            A. M. Andrus, Code ST

National Aeronautics & Space Administration
Scientific and Technical Information Facility
P.O. Box 5700
Bethesda, Maryland 20014 (2 copies + 1 reproducible)

National Aeronautics & Space Administration
Goddard Space Flight Center
Greenbelt, Maryland 20771
Attention: Thomas Hennigan, Code 632.2

National Aeronautics & Space Administration
Langley Research Center
Langley Station
Hampton, Virginia 23365
Attention: S. T. Peterson

National Aeronautics & Space Administration
Lewis Research Center
21000 Brookpark Road
Cleveland, Ohio 44135
Attn: B. Lubarsky, Mail Stop 500-201
       R. L. Cummings, Mail Stop 500-201
       H. J. Schwartz, Mail Stop 500-201
       J. E. Dilley, Mail Stop 500-309
       N. D. Sanders, Mail Stop 302-1
       M. J. Saari, Mail Stop 500-202
       R. R. Miller, Mail Stop 500-202
       Technology Utilization Office, Mail Stop 3-16
       (Project Manager), Solar & Chemical Power Branch
                       Mail Stop 500-201
                          (1 copy + 1 reproducible)
       Library, Mail Stop 3-7
       Report Control, Mail Stop 5-5

National Aeronautics & Space Administration
Marshall Space Flight Center
Huntsville, Alabama 35812
Attention: Philip Youngblood and R. Boehme

National Aeronautics & Space Administration
Ames Research Center
Moffett Field, California 94035
  Mountain View
Attention: James R. Swain, Pioneer Project

National Aeronautics & Space Administration
Ames Research Center
Moffett Field, California 94035
  Mountain View
Attention: Mr. T. Wydeven
            Environmental Control Branch

National Aeronautics & Space Administration
Ames Research Center
Moffett Field, California 94035
  Mountain View
Attention: Jon Rubenzer, Biosatellite Project

National Aeronautics & Space Administration
Manned Spacecraft Center
Houston, Texas 77058
Attention: Richard Ferguson (EP-5)
            Robert Cohen, Gemini Project Office
            F. E. Eastman (EE-4)

National Aeronautics & Space Administration
Western Operations Office
Santa Monica, California 90406
Attention: P. Pomerantz

Jet Propulsion Laboratory
4800 Oak Grove Drive
Pasadena, California 91103
Attention: Aiji Uchiyama

DEPARTMENT OF THE ARMY

U. S. Army Engineer R & D Labs.
Fort Belvoir, Virginia 22060
Attention: Dr. Galen Frysinger (Code SMOFB-EP)
            Electrical Power Branch

U. S. Army Electronics R & D Labs.
Fort Monmouth, New Jersey
Attention: Arthur F. Daniel (Code SELRA/SL-PS)
            David Linden   (Code SELRA/SL-PS)

U.S. Army Electronics R & D Labs.
Fort Monmouth, New Jersey
Attention: Dr. Adolph Fischbach (Code SELRA/SL-PS)
            Dr. H. F. Hunger (Code SELRA/SL-PS)

Research Office
R & D Directorate
Army Weapons Command
Rock Island, Illinois
Attn: Mr. G. Riensmith, Chief

U. S. Army Research Office
Chief, Rand D.
Department of the Army
3D442, The Pentagon
Washington, D. C. 20546
Attention: Dr. Sidney J. Mangram

U. S. Army Research Office
Physical Sciences Division
3045 Columbia Pike
Arlington, Virginia

Harry Diamond Labs.
Room 300, Building 92
Connecticut Avenue & Van Ness Street, N.W.
Washington, D. C.
Attention: Nathan Kaplan

Army Materiel Command
Research Division
AMCRD-RSCM T-7
Washington 25, D. C.
Attention: John W. Crellin

Natick Labs.
Clothing & Organic Materials Division
Natick, Massachusetts
Attention: Leo A. Spano

Natick Labs.
Clothing & Organic Materials Division
Natick, Massachusetts
Attention: Robert N. Walsh

U. S. Army Research Office
Box CM, Duke Station
Durham, North Carolina
Attention: Paul Greer

U. S. Army Research Office
Box CM, Duke Station
Durham, North Carolina
Attention: Dr. Wilhelm Jorgensen

U. S. Army Mobility Command
Research Division
Center Line, Michigan 48090
Attention: O. Renius (AMSMO-RR)

Hq., U. S. Army Materiel Command
Development Division
Washington 25, D. C.
Attention: Marshall D. Aiken (AMCRD-DE-MO-P)

DEPARTMENT OF THE NAVY

Office of Naval Research
Department of the Navy
Washington 25, D. C.
Attention: Dr. Ralph Roberts, Code 429
            Head, Power Branch

Office of Naval Research
Department of the Navy
Washington 25, D. C.
Attention: H. W. Fox, Code 425

Bureau of Naval Weapons
Department of the Navy
Washington 25, D. C.
Attention: Milton Knight, Code RAAE-50

Bureau of Naval Weapons
Department of the Navy
Washington 25, D. C.
Attention: Whitwell T. Beatson, Code RAAE-52

U. S. Naval Research Laboratory
Washington, D. C. 20390
Attention: Dr. J. C. White, Code 6160

Bureau of Ships
Department of the Navy
Washington 25, D. C.
Attention: Bernard B. Rosenbaum, Code 340

Bureau of Ships
Department of the Navy
Washington 25, D. C.
Attention: C. F. Viglotti, Code 660

Naval Ordnance Laboratory
Department of the Navy
Corona, California
Attention: William C. Spindler (Code 441)

Naval Ordnance Laboratory
Departmentof the Navy
Silver Spring, Maryland
Attention: Philip B. Cole (Code WB)

DEPARTMENT OF THE AIR FORCE

Flight Vehicle Power Branch
Air Force Aero Propulsion Laboratory
Wright-Patterson Air Force Base, Ohio
Attention: J. E. Cooper (Code APIP)

Space Systems Division
Los Angeles Air Force Station
Los Angeles, California, 90045
Attention: SSSD

AF Cambridge Research Lab.
Attention: CRZE
L. C. Hanscom Field
Bedford, Massachusetts
Attention: Francis X. Doherty

AF Cambridge Research Lab.
Attention: CRZE
L. C. Hanscom Field
Bedford, Massachusetts
Attention: Edward Raskind (Wing F)

Rome Air Development Center, RSD
Griffiss AFB, New York 13442
Attention: Frark J. Mollura (RASSM)

ATOMIC ENERGY COMMISSION

Army Reactors, DRD
U. S. Atomic Energy Commission
Washington 25, D. C.
Attention: D. B. Hoatson

OTHER GOVERNMENT AGENCIES

Office, DDR&E: USW & BSS
The Pentagon
Washington 25, D. C.
Attention: G. B. Wareham

Staff Metallurgist
Office, Director of Metallurgy Research
Bureau of Mines
Interior Building
Washington, D. C. 20240
Attention: Kenneth S. Higbie

Institute for Defense Analyses
Research and Engineering Support Division
400 Army-Navy Drive
Arlington, Virginia 22202
Attention: Dr. George C. Szego

Institute for Defense Analyses
Research and Engineering Support Division
400 Army-Navy Drive
Arlington, Virginia 22202
Attention: R. Hamilton

Power Information Center
University of Pennsylvania
Moore School Building
200 South 33rd Street
Philadelphia 4, Pennsylvania

Office of Technical Services
Department of Commerce
Washington, D. C. 20009

PRIVATE INDUSTRY

Aeronutronic Division
Philco Corporation
Ford Road
Newport Beach, California 92663
Attention: Dr. S. W. Weller

Alfred University
Alfred, New York
Attention: Prof. T. J. Gray

Allis-Chalmers Mfg. Company
1100 South 70th Street
Milwaukee, Wisconsin 53201
Attention: Mr. John Plattner

Allison Division
General Motors Corporation
Indianapolis 6, Indiana
Attention: Dr. Robert B. Henderson

American Machine & Foundry
689 Hope Street
Springdale, Connecticut
Attention: Dr. L. H. Shaffer
            Research & Development Division

Arthur D. Little, Inc.
Acorn Park
Cambridge, Mass., 02140
Attention: Dr. Ellery W. Stone

Astropower, Incorporated
Douglas Aircraft Company, Inc.
2121 College Drive
Newport Beach, California
Attention: Dr. Carl Berger

Atomics International, Division of
North American Aviation, Inc.
Canoga Park, California
Attention: Dr. H. L. Recht

Battelle Memorial Institute
505 King Avenue
Columbus, Ohio 43201
Attention: Dr. C. L. Faust

Bell Telephone Laboratories, Inc.
Murray Hill, New Jersey
Attention: Mr. U. B. Thomas

Clevite Corporation
Mechanical Research Division
540 East 105th Street
Cleveland, Ohio 44108
Attention: A. D. Schwope

Electrochimica Corporation
1140 O'Brien Drive
Menlo Park, California
Attention: Dr. Morris Eisenberg

Electro-Optical Systems, Inc.
300 North Halstead Street
Pasadena, California
Attention: E. Findl

Engelhard Industries, Inc.
497 DeLancy Street
Newark 5, New Jersey
Attention: Dr. J. G. Cohn

Esso Research & Engineering Company
Products Research Division
P. O. Box 121
Linden, New Jersey 07036
Attention: Dr. Robert Epperly

The Franklin Institute
Benjamin Franklin Avenue at 20th St.
Philadelphia 3, Pennsylvania
Attention: Robert Goodman

Garrett Corporation
1625 Eye Street, N. W.
Washington 6, D. C.
Attention: George R. Sheperd

General Electric Company
Direct Energy Conversion Operations
Lynn, Massachusetts
Attention: Dr. E. Oster

General Electric Company
Missile & Space Vehicle Department
P. O. Box 8555
Philadelphia, Pennsylvania 19101
Attention: E. W. Kipp, Room T-2513

General Electric Company
Research Laboratory
Schenectady, New York
Attention: Dr. H. Liebhafsky

General Motors Corporation
Box T
Santa Barbara, California
Attention: Dr. C. R. Russell

General Motors Corporation
Research Laboratories
Electrochemistry Department
12 Mile & Mound Roads
Warren, Michigan 48090
Attention: Mr. Seward Beacom

G. M. Defense Research Lab.
P. O. Box T
Santa Barbara, California
Attention: Dr. Smatko

Globe-Union, Inc.
900 East Keefe Avenue
Milwaukee, Wisconsin 53201
Attention: Dr. W. Towle

Hughes Research Laboratories Corp.
Malibu, California
Attention: T. M. Hahn

Institute of Gas Technology
State & 34th Streets
Chicago, Illinois
Attention: Mr. Bernard Baker

Ionics, Incorporated
152 Sixth Street
Cambridge, Massachusetts 02142
Attention: Dr. Werner Glass

John Hopkins University
Applied Physics Laboratory
8621 Georgia Avenue
Silver Spring, Maryland
Attention: W. A. Tynan

Leesona Moos Laboratories
Lake Success Park
Community Drive
Great Neck, New York
Attention: Dr. A. Moos

Midwest Research Institute
425 Volker Boulevard
Kansas City 10, Missouri
Attention: Dr. B. W. Beadle

Monsanto Research Corporation
Everett, Massachusetts 02149
Attention: Dr. J. Smith

North American Aviation Inc.
S&ID Division
Downey, California
Attention: Dr. James Nash

Power Sources Division
Whittaker Corporation
9601 Canoga Avenue
Chatsworth, California 91311
Attention: Dr. M. Shaw

Pratt & Whitney Aircraft Division
United Aircraft Corporation
East Hartford 8, Connecticut
Attention: Librarian

Radio Corporation of America
Astro Division
Heightstown, New Jersey
Attention: Dr. Seymour Winkler

Rocketdyne
6633 Canoga Avenue
Canoga Park, California
Attention: Library, Dept. 586-306

Space Technology Laboratories, Inc.
2400 E. El Segundo Boulevard
El Segundo, California
Attention: Dr. A. Krauz

Speer Carbon Company
Research & Development Laboratories
Packard Road at 47th Street
Niagara Falls, New York
Attention: Dr. L. M. Liggett

Stanford Research Institute
820 Mission Street
South Pasadena, California
Attention: Dr. Fritz Kalhammer

Texas Instruments, Inc.
13500 North Central Expressway
Dallas, Texas
Attention: Mr. Isaac Trachtenberg

Thiokol Chemical Corporation
Reaction Motors Division
Denville, New Jersey
Attention: Dr. D. J. Mann

Thompson Ramo Wooldridge, Inc.
23555 Euclid Avenue
Cleveland, Ohio 44117
Attention: Librarian

Tyco Laboratories, Inc.
Bear Hill
Waltham 54, Mass.
Attention: W. W. Burnett

University of Pennsylvania
Philadelphia, Pennsylvania 19104
Attention: Prof. John O'M. Bockris

University of Pennsylvania
Philadelphia, Pennsylvania 19104
Attention: Dr. Manfred Altman

Unified Science Associates, Inc.
826 South Arroyo Parkway
Pasadena, California
Attention: Dr. Sam Naiditch

Union Carbide Corporation
12900 Snow Road
Parma, Ohio
Attention: Dr. George E. Evans

University of California
Space Science Laboratory
Berkeley 4, California
Attention: Prof. Charles W. Tobias

Western Reserve University
Cleveland, Ohio
Attention: Prof. Ernest Yeager

Westinghouse Electric Corporation
Research and Development Center
Churchill Borough
Pittsburgh, Pennsylvania
Attention: Dr. A. Langer

Yardney Electric Corporation
40-50 Leonard Street
New York, New York
Attention: Dr. Paul Howard

The Western Company
Suite 802 RCA Building
Washington, D. C.
Attention: R. T. Fiske

Johns-Manville R & E Center
P. O. Box 159
Manville, New Jersey
Attention: Mr. J. S. Parkinson